Long-term controls on ocean phosphorus and oxygen in a global biogeochemical model

V. Palastanga,[1] C. P. Slomp,[1] and C. Heinze[2,3,4]

Received 24 March 2010; revised 23 October 2010; accepted 13 June 2011; published 21 September 2011.

[1] In this study, we use a biogeochemical ocean general circulation model (HAMOCC), originally developed for the carbon and silicon cycles, and expand it with a description of the sedimentary phosphorus (P) cycle. The model simulates the release of reactive P by aerobic and anaerobic degradation of organic matter in the sediment, as well as formation and burial of Fe-oxide bound P and authigenic Ca-P minerals. We also include pre-anthropogenic inputs of P from atmospheric dust, which is mostly in the form of detrital apatite. Model predicted total P concentrations and rates of reactive P burial for the deep sea agree reasonably well with observations in open ocean and near continental margin sediments. As part of a sensitivity analysis, we assess the long-term response of ocean productivity and deep water oxygenation to increases in the riverine input of P and preferential release of P from sediments. The simulations show that the feedback from preferential P regeneration accelerates the expansion of suboxia ($O_2 < 25$ μM) along continental margins and in the naturally suboxic areas in tropical-subtropical regions on timescales of 10–100 ka. For a case in which maximum P regeneration from sediments is enabled, a large-scale pattern of bottom water suboxia (30% of the total ocean area) develops over the southeastern, tropical and northern Pacific Ocean sectors.

Citation: Palastanga, V., C. P. Slomp, and C. Heinze (2011), Long-term controls on ocean phosphorus and oxygen in a global biogeochemical model, *Global Biogeochem. Cycles*, *25*, GB3024, doi:10.1029/2010GB003827.

1. Introduction

[2] Phosphorus (P) is an essential nutrient in marine biogeochemistry. P is often regarded as the 'ultimate limiting nutrient', because it is the external input of P that regulates global ocean productivity on long timescales, while nitrogen acts as the instantaneous limiting nutrient [*Tyrrell*, 1999]. Therefore, detailed insight into the processes that control the oceanic P inventory is needed for a correct understanding of the links between primary productivity, global biogeochemical cycling and climate on geological timescales.

[3] The major source of P to the ocean is river input and the major sink is burial in sediments. Most P is buried in sediments in the form of either organic P, authigenic carbonate fluorapatite (hereafter called authigenic Ca-P) or Fe-oxide bound P [*Ruttenberg*, 1993; *Delaney*, 1998]. The efficiency of reactive P burial is strongly influenced by bottom water redox conditions. More specifically, P is more easily regenerated when bottom waters are anoxic [*Ingall and Jahnke*, 1994; *Slomp and Van Cappellen*, 2007]. As a consequence, an initial increase in primary production, leads to increased respiration in the water column and more oxygen depleted waters, which in turn stimulates benthic release of P and productivity, in a positive feedback loop [*Van Cappellen and Ingall*, 1994; *Slomp and Van Cappellen*, 2007]. Various box model studies suggest that this feedback loop played a major role in sustaining marine productivity and black shale formation during Cretaceous Oceanic Anoxic events (OAEs) [*Handoh and Lenton*, 2003; *Nederbragt et al.*, 2004; *Tsandev and Slomp*, 2009]. *Handoh and Lenton* [2003] showed that a moderate increase in P weathering can trigger self-sustained oscillations of the P and oxygen coupled biogeochemical cycles on the timescales of OAEs if the positive feedback from P regeneration is strong. The results of *Tsandev and Slomp* [2009] imply that a decrease in oceanic ventilation is a further requirement for global scale deep sea anoxia. In their model, a moderate increase in river input of P can cause oxygen depletion in the deep sea over long timescales, if a mechanism for enhanced P recycling from the sediment is present and circulation is reduced compared to the present-day. The modeling study of *Wallmann* [2003] demonstrated that the onset of ocean anoxia may be highly non-linear, with the anoxia-productivity feedback becoming most important below a threshold in deep water oxygen concentration of 100 μM. In the model simulations, both eutrophic conditions and anoxia spread rapidly as this threshold is overcome.

[4] Recent measurements and model simulations indicate decreasing concentrations of dissolved oxygen in various regions of the world ocean over the past decades which have been mainly linked to changes in oxygen solubility and

[1]Department of Earth Sciences-Geochemistry, Faculty of Geosciences, Utrecht University, Utrecht, Netherlands.
[2]Geophysical Institute, University of Bergen, Bergen, Norway.
[3]Bjerknes Centre for Climate Research, Bergen, Norway.
[4]Uni Bjerknes Centre, Uni Research, Bergen, Norway.

0886-6236/11/2010GB003827

ventilation of ocean waters induced by global warming [*Whitney et al.*, 2007; *Stramma et al.*, 2008]. Simulations with Earth System Models predict a further expansion of ocean oxygen depletion in response to global changes in water column conditions associated with continued anthropogenic CO_2 release [*Shaffer et al.*, 2009]. The oxygen depletion is further amplified upon changes in C:N ratios of marine biota [*Oschlies et al.*, 2008], changes in carbon export to the deep ocean upon ocean acidification [*Hofmann and Schellnhuber*, 2009] and a decrease in ocean circulation [*Shaffer et al.*, 2009]. Model results also predict a variable response of different ocean regions to anthropogenic forcing, with current suboxic areas in the Indian and Pacific ocean likely to be most affected on millennial timescales [*Hofmann and Schellnhuber*, 2009].

[5] Current biogeochemical ocean general circulation models for the open ocean do not include a description of the sedimentary P cycle and thus do not allow an assessment of the role of preferential regeneration of P from sediments on ocean oxygenation on timescales of tens of millennia. In addition, potential changes in river inputs of P due to enhanced chemical weathering upon global warming [*Gislason et al.*, 2009] are not considered in these models.

[6] In this study, we investigate the effect of increased inputs of P from rivers and redox dependent burial of P on ocean productivity and deep water oxygenation on a timescale of up to 200 ka. We analyze the coupled response of the marine C, P and oxygen cycles to climate changes on timescales of several hundred thousand years, while longer variability in the geological record is ignored. We use the version of the Hamburg Oceanic Carbon Cycle model (HAMOCC) for long-term simulations [*Heinze et al.*, 1999], which we expand to include anaerobic degradation of organic matter in the sediment and formation and burial of Fe-oxide bound P and authigenic Ca-P minerals. In addition to the supply of P from rivers, we include inputs of P from mineral dust. Although anthropogenic sources of atmospheric P might be significant [*Mahowald et al.*, 2008], these are not considered in this preindustrial model study. Total sediment P concentrations are compared to observations from the literature. The input of P from rivers is varied and the long-term, coupled response of oceanic primary productivity, ocean oxygenation and preferential regeneration of P from sediments is assessed. Our results show that increases in P delivery from rivers relative to preindustrial values together with enhanced recycling of P from sediments promote the expansion of tropical suboxic volumes (oxygen concentrations <25 μM) on timescales from 10 to 100 ka. Ultimately, the simulations show that enhanced P availability may lead to the development of bottom water suboxia.

2. Model Description

2.1. HAMOCC2

[7] In this study, we use the HAMOCC model [*Maier-Reimer*, 1993] in its annually averaged version [*Heinze et al.*, 1999, 2003, 2006], which was specifically developed for long-term integrations. The physical model has a horizontal resolution of 3.5° × 3.5° and 11 layers for the oceanic water column (centered around 25, 75, 150, 250, 450, 700, 1000, 2000, 3000, 4000 and 5000 m). The circulation is fixed and is based on the velocity and thermohaline fields of the Hamburg Large-Scale Geostrophic ocean general circulation model [*Maier-Reimer et al.*, 1993]. In addition to the ocean reservoir, the biogeochemical model includes the bioturbated sediment, with a layer thickness of 10 cm separated into 11 sublayers (centered around 0.3, 0.45, 1.35, 1.85, 2.6, 3.6, 4.6, 6.325, and 8.775 cm), and a zonally mixed atmosphere compartment. Model tracers in the water column are total alkalinity, total CO_2 (equivalent to dissolved inorganic carbon, DIC), phosphate (PO_4), oxygen (O_2), dissolved organic carbon (DOC), and silicic acid, and in the sediment pore waters, the same tracers as in the water column (except for DOC). Gas transfer of O_2 and CO_2 is enabled at the air-sea interface. Prognostic solid variables include calcium carbonate, opal, particulate organic carbon (POC), and clay in the water column as well as in the bioturbated sediment. Export production of biogenic particles is modeled in the surface layer, with PO_4 as the only limiting nutrient in the model. For a full description of the formulation used for biological export production, the particle flux through the water column, pore water chemistry and pore water diffusion, we refer to *Heinze et al.* [2003]. Because of the coarse spatial resolution, continental margin processes are not explicitly represented. In the next section, we describe the modifications made in the model to include anaerobic degradation of organic matter, and a full description of the sedimentary P cycle. A schematic of the model P cycle is shown in Figure 1.

2.2. New Parameterization for POC Mineralization

[8] In the original version of the model, the oxidation of organic carbon in the sediment was assumed to be directly proportional to the pore water oxygen concentration (see *Heinze et al.* [2003]). However, anaerobic respiration is important both in continental margin and deep sea regions with high rates of organic matter deposition [*Tromp et al.*, 1995; *Middelburg et al.*, 1997]. To account for anaerobic degradation of organic matter in the model, we add an anoxic pathway that becomes active when oxygen falls below a critical level, O_{2crit}. Further, we assume that the total rate of POC degradation is subject to linear Monod kinetics [*Van Cappellen and Wang*, 1996], thus aerobic degradation is independent of the oxygen concentration in the oxic part of the sediment and it comes to a halt when oxygen is nearly depleted, while anaerobic degradation is not limited by oxidant availability. Secondary redox reactions involving reduced substances are not included. Therefore, the net rate of POC degradation (G_C) is expressed as

$$G_C = G_{Cox} = k_{ox} POC \qquad \text{if } O_2 > O_{2crit} \tag{1a}$$

$$G_C = G_{Cox} + G_{Cax} = k_{ox} POC \frac{[O_2]}{O_{2crit}} + k_{ax} POC \qquad \text{if } O_2 < O_{2crit} \tag{1b}$$

where G_{Cox} and G_{Cax} represent the aerobic and anaerobic rate of POC degradation (in units of mol C L^{-1} a^{-1}), POC is the concentration of particulate organic C (expressed in mol L^{-1}), k_{ox} is the first-order kinetic constant for aerobic POC mineralization (a^{-1}), k_{ax} is the first-order kinetic constant for anaerobic POC mineralization (a^{-1}), and O_2 is the pore water oxygen concentration (mol L^{-1}).

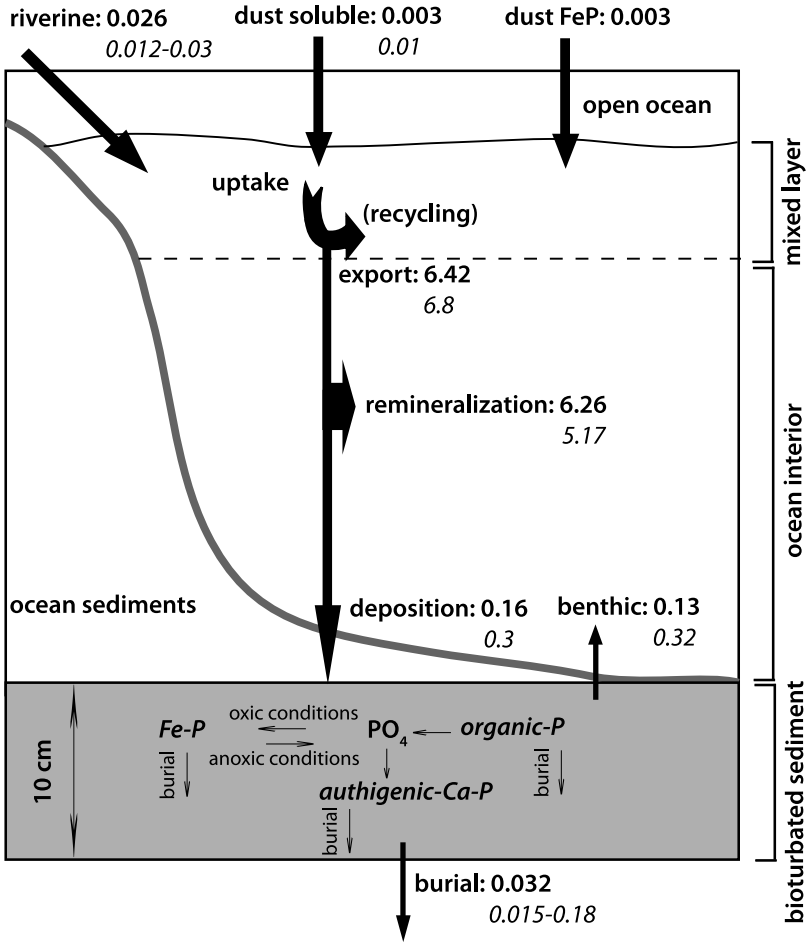

Figure 1. Schematic of the global biogeochemical cycling of P, including a description of sedimentary P dynamics. Arrows indicate the flow of P (dissolved or particulate) in units of Tmol P a^{-1}. Values of the fluxes as resulting from the model reference run are shown in bold; these are compared with estimates from observations (italics) of the pre-anthropogenic input of P from rivers [*Wheat et al.*, 1996; *Harrison et al.*, 2005]; aeolian supply of dissolved P, organic P deposition, and benthic P regeneration [*Delaney*, 1998]. The range of P burial shows an estimate for the deep-sea and the global high end estimate from work by *Ruttenberg* [1993]. Estimates for the export of P from the surface layer and P remineralization in the water column are obtained from the associated fluxes of particulate organic C [*Dunne et al.*, 2007], assuming a C:P ratio of 117 [*Anderson and Sarmiento*, 1994]. The flux of iron-bound P (Fe-P) from atmospheric dust which is deposited into the sediments is a model assumption. Hydrothermal activity is not represented in the model. The sediment module (10 cm thick) is drawn with an expanded vertical scale for clarity. The P diagenetic processes included in the model are degradation of organic P, precipitation of authigenic carbonate fluorapatite (Ca-P), formation of Fe-P in oxic sediments, and Fe-P dissolution in anoxic sediments. The model simulates mixing and burial of sediment solid phases.

[9] First-order kinetic constants for aerobic and anaerobic POC degradation (k_{ox} and k_{ax}) show a wide range of variability for different depositional environments [*Tromp et al.*, 1995]. Values for k_{ox} fall in the range of 0.001–0.01 a^{-1} in pelagic sediments [*Emerson and Hedges*, 1988; *Tromp et al.*, 1995], and are in general higher than 0.01 a^{-1} in continental margin sediments [*Tromp et al.*, 1995]. Here, values of these parameters are selected according to the best fit to global surface POC observations [*Seiter et al.*, 2004]. As in the model relatively shallow continental shelves with high POC deposition rates are delineated by the 2000 m isobath (Figure 2a), we consider a value for k_{ox} equal to 0.01 a^{-1} for the regions with water depths <2000 m, hereafter referred as margin (sediments), and 0.005 a^{-1} for depths >2000 m, hereafter referred as deep sea (sediments). Anaerobic degradation rates are set to relatively lower values in both regions. Rates of sediment mixing by macrofauna (D_b) are set to 0.3 cm^2 a^{-1} for $z > 3000$ m and to 1.0 cm^2 a^{-1} for $z < 3000$ m according to estimates from *Tromp et al.* [1995].

2.3. Sedimentary P Cycle

[10] Organic matter deposition from the water column is the main source of P to sediments. Upon reaching the sediment, most of the organic matter is degraded (in open ocean settings up to 99.6% [*Seiter et al.*, 2005]), and the P is released to pore waters. Here P can be scavenged by sorption to iron oxides

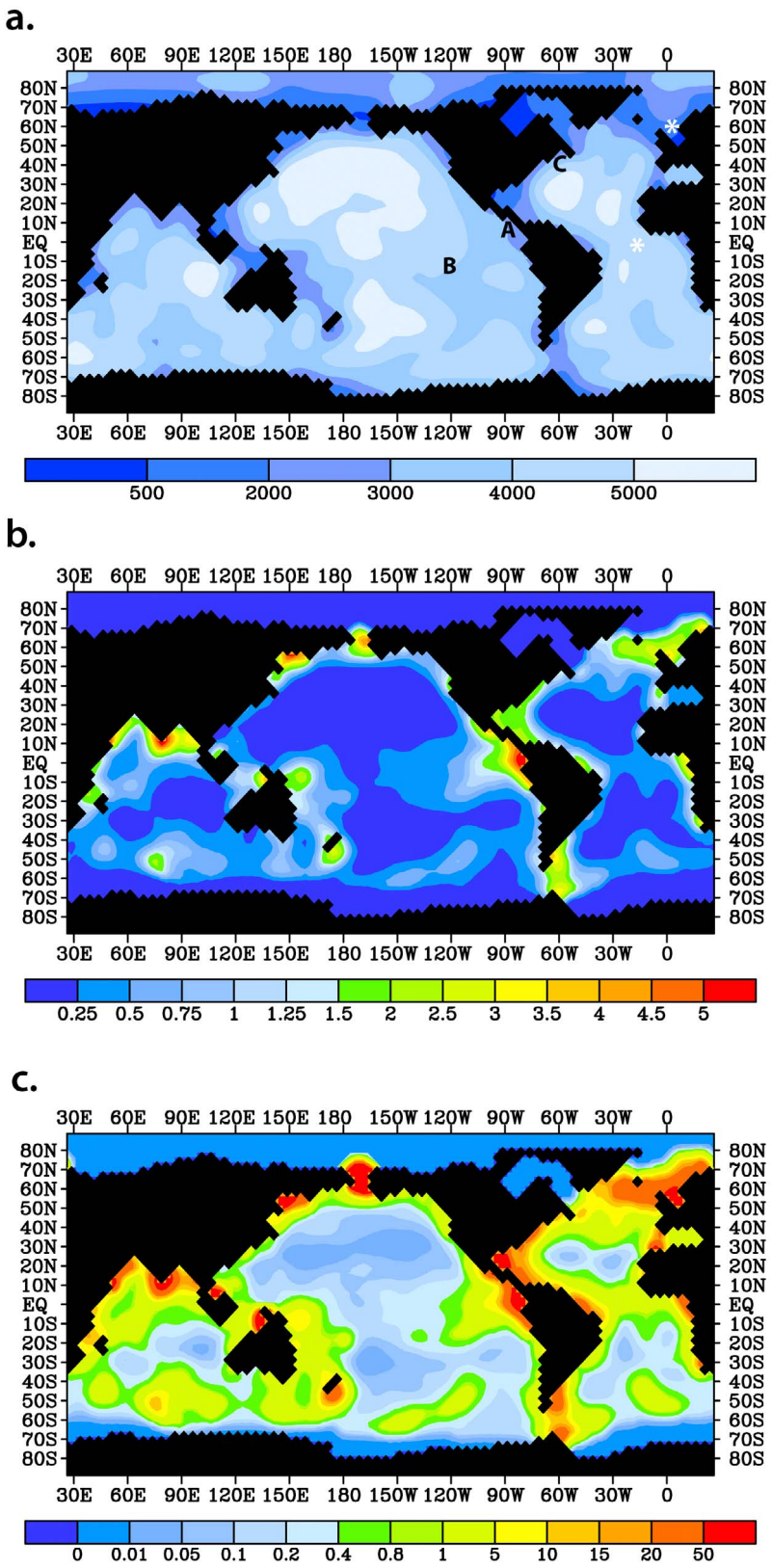

Figure 2. (a) The model bottom topography (m). The letters A, B, and C denote the locations of the POC profiles shown in Figure 4. The white stars indicate the two locations selected to depict the profiles of Figure 7. (b) Sediment POC averaged over the entire bioturbated layer (wt%) and (c) POC accumulation rates (mmol C m^{-2} a^{-1}), as simulated in the model reference run.

(Fe-P) in the oxic part of the sediment, can re-precipitate as authigenic Ca-P, or can be released back to the water column [*Ruttenberg and Berner*, 1993; *Filippelli and Delaney*, 1996; *Slomp et al.*, 1996; *Anderson et al.*, 2001]. Thus, to represent the cycling of P in sediments, we consider two additional reactive P solid phases (Fe-P and authigenic Ca-P) besides organic P, which is included in the original version of HAMOCC. We also add a detrital apatite phase of atmospheric origin [*Ruttenberg and Berner*, 1993].

[11] Originally, particulate organic P (POP) and POC in the model were linked by a constant Redfield ratio assumed to be [1:122]. The latter is obtained from a revision of the traditional Redfield ratio using thermocline data and oxygen utilization ratios significantly higher than Redfield's values [*Takahashi*, 1985]. In the present approach, POP is treated as a prognostic sediment variable subject to degradation, transport and burial as POC. To simulate preferential regeneration of P from organic matter under anoxic conditions, i.e. for $O_2 < O_{2crit}$, we introduce an acceleration factor (α) in the anaerobic degradation rate of POP (G_{Pax}), which based on Monod linear kinetics reads

$$G_{Pax} = \alpha k_{ax} POP \tag{2}$$

where POP is the concentration of particulate organic P (expressed in mol L^{-1}) and k_{ax} is the first-order kinetic constant for anaerobic POC mineralization. Values of the parameter α may typically vary between 1 and 3 [*Wallmann*, 2003]. The sensitivity of the model results to different parameter values for preferential P regeneration is explored in Section 5.

[12] Scavenging of P to ferric iron oxides is a prominent process in near coastal sediments where iron oxides delivered from rivers are abundant [*Krom and Berner*, 1980], and along mid-ocean ridges as iron is released to the water column with hydrothermal plume particles [*Wheat et al.*, 1996]. The hydrothermal flux of P to the sediments is about 0.008 TmolP a^{-1} [*Delaney*, 1998]; however, hydrothermal activity is not represented in the present model. Reactive P might also be scavenged by iron rich dust particles both in the atmosphere and water column [*Delaney*, 1998]. The process of P scavenging to particulate matter in the water column is not explicitly modeled here, but we consider an input of Fe-P derived from the atmospheric dust field (see explanation below). The scavenging of P to Fe-oxides that leads to the formation of Fe-P in the oxic sediment layer, i.e. for $O_2 > O_{2crit}$, is modeled as a first order rate process [*Slomp et al.*, 1996; *Gypens et al.*, 2008], with the rate of P sorption (R_s) given by

$$R_s = k_s(PO_4 - C_s) \tag{3}$$

where k_s is the rate constant for P sorption (a^{-1}), PO_4 is the pore water phosphate concentration (mol L^{-1}), and C_s is the equilibrium concentration for P sorption. We use k_s equal to 36.5 a^{-1} and C_s equal to 2.0 μmol L^{-1} in margin sediments based on the range of observations from North Atlantic shallow sediments [*Slomp et al.*, 1996]. Values of these parameters in the deep sea are fitted for this study to simulate lower rates of in situ P sorption relative to margins; thus k_s has a value of 3.65 a^{-1} and C_s is 12.0 μmol L^{-1} (Table 1).

[13] The release of P due to reductive dissolution of Fe-oxides in the anoxic sediment layer follows the desorption rate (R_m),

$$R_m = k_m(FeP - M_f) \tag{4}$$

where FeP represents the concentration of Fe-P in the sediment (expressed in units of mol L^{-1}), k_m is the rate constant for P release upon Fe-oxide dissolution (a^{-1}), and M_f is the minimum concentration of Fe-P required for the release of P. Since the rate of reductive dissolution of Fe-oxides is partly determined by the activity of sulfate reducing bacteria [*Boudreau*, 1997], k_m is approximated as a background value (0.05 a^{-1}) plus a rate dependent on the anaerobic degradation rate of POC, i.e. $k_m = 0.05 + k_0(G_{Cax}^2/G_C\overline{G_{Cax}})$, where k_o is the constant rate of Fe-oxides dissolution obtained by model fitting of North Atlantic slope sediments [*Slomp et al.*, 1996], G_C is the total rate of POC degradation in the model (equation (1)), G_{Cax} is the modeled anaerobic rate of POC degradation (equation (1b)), and $\overline{G_{Cax}}$ is the global spatial average of G_{Cax} computed in each layer of the bioturbated sediment. Thus, the ratio $G_{Cax}/\overline{G_{Cax}}$ measures the relative importance of anaerobic POC degradation at each grid point per layer in the sediment. Values for the minimum concentration M_f are fitted for this study, with M_f equal to 2.0 μmol g^{-1} (dry weight) in deep sea sediments and to zero in margin sediments.

[14] The formation of uniformly dispersed authigenic Ca-P is considered a first-order process in the bioturbated sediment [*Van Cappellen and Berner*, 1988]. Thus, if the pore water PO_4 concentration exceeds a saturation value, precipitation of authigenic Ca-P occurs according to the rate

$$R_a = k_a(PO_4 - C_a) \tag{5}$$

where k_a is the rate constant for Ca-P precipitation (a^{-1}), PO_4 is the pore water phosphate concentration, and C_a is the equilibrium concentration for Ca-P precipitation. Values of k_a are still poorly constrained either from observations or diagenetic model calculations. *Van Cappellen and Berner* [1988] proposed a range for k_a from 0.01 to 10 a^{-1} for simulations of dispersed authigenic Ca-P formation in upwelling continental margins. We choose k_a equal to the value found by model fits in North Atlantic continental slope sediments, i.e. 0.37 a^{-1} [*Slomp et al.*, 1996]. The equilibrium constant C_a is set to a uniform value of 3.7 10^{-3} μmol L^{-1} based on the relationship from *Atlas and Pytkowicz* [1977].

[15] It is well recognized that aeolian supply of P becomes relatively important away from continental margins, and might be relevant for primary productivity in oligotrophic regions [*Benitez-Nelson*, 2000; *Mahowald et al.*, 2008]. In this study, we estimate the input of atmospheric P using the mineral dust field simulated by the model of *Andersen et al.* [1998]. Other sources of atmospheric P, including anthropogenic effects [*Mahowald et al.*, 2008], are not considered. We assume a concentration of 0.09 wt% for P in dust, which is in the range of atmospheric P concentrations measured in different desert areas, i.e. between 0.05 and 0.13 wt% [*Mahowald et al.*, 2008]. Global measurements of atmospheric P solubility are still scarce and considerably uncertain [*Baker et al.*, 2006]. Overall, the solubility of

Table 1. Standard Values of Parameters Used in the Reference Run

Parameter/Symbol	Value
Rate constant for aerobic degradation of sediment POC (margins), k_{ox}	0.01 a^{-1}
Rate constant for aerobic degradation of sediment POC (deep sea), k_{ox}	0.005 a^{-1}
Rate constant for anaerobic degradation of sediment POC (margins), k_{ax}	0.008 a^{-1}
Rate constant for anaerobic degradation of sediment POC (deep sea), k_{ax}	0.002 a^{-1}
Oxygen saturation concentration for the redox boundary, O_{2crit}	5.0 μ mol L^{-1}
Parameter for preferential regeneration of P relative to C, α	2.0
Bioturbation coefficient (z < 3000m), D_b	1.0 cm^2 a^{-1}
Bioturbation coefficient (z > 3000m), D_b	0.3 cm^2 a^{-1}
Rate constant for P sorption (margins), k_s	36.5 a^{-1}
Rate constant for P sorption (deep sea), k_s	3.65 a^{-1}
Equilibrium concentration for P sorption (margins), C_s	2.0 μmol L^{-1}
Equilibrium concentration for P sorption (deep sea), C_s	12 μ mol L^{-1}
Rate of reductive dissolution of Fe-P (constant value), k_o	0.19 a^{-1}
Asymptotic concentration for Fe-P dissolution (margins), M_f	0.0 μ mol g^{-1}
Asymptotic concentration for Fe-P dissolution (deep sea), M_f	2.0 μ mol g^{-1}
Rate constant for authigenic Ca-P precipitation, k_a	0.37 a^{-1}
Phosphate equilibrium concentration for Ca-P precipitation, C_a	3.7 μ mol L^{-1}
Global river input of PO_4	$0.026 \cdot 10^{12}$ mol P a^{-1}
Atmospheric (dust) input of PO_4	$0.003 \cdot 10^{12}$ mol P a^{-1}
Atmospheric (dust) input of clays	0.6 Gt a^{-1}
Continental (rivers) input of clays (z < 500 m)	3.5 Gt a^{-1}
Continental (rivers) input of clays (z > 500 m)	0.7 Gt a^{-1}

atmospheric P varies with the origin of the source material [*Mahowald et al.*, 2008]. For instance, P solubility in Saharan dust close to the African coast is lower, e.g. 8–10% [*Graham and Duce*, 1979] than at open ocean locations, where a range of 20–50% is reported [*Graham and Duce*, 1979; *Baker et al.*, 2006]. Here we consider that 20% of atmospheric P is bioavailable in the surface ocean layer, except in the Mediterranean Sea and tropical North Atlantic region, where a solubility of 10% is used. There is no further desorption of P from dust particles below the surface, and the sinking flux of atmospheric P is ultimately deposited into the sediment. Up-to-date, there is very little data on the speciation of atmospheric P. Extraction of P in a sample of Saharan dust in the eastern Mediterranean revealed a fractionation of 43% authigenic Ca-P, 22% Fe-P, 12% organic P and 12% detrital P [*Eijsink et al.*, 2000]. For this study, we assume that the latter speciation is valid in oceanic regions where the model atmosphere is very dusty (i.e. dust deposition rates $>5 \times 10^{-4}$ g cm^{-2} a^{-1}). In the remaining regions, we adopt a fractionation of atmospheric P equal to 78% detrital apatite and 22% Fe-P. The prescribed input of Fe-P from the atmosphere (a total of 0.003 Tmol P a^{-1}) is aimed to represent the flux of P scavenged to iron rich dust particles either in the atmosphere or the water column, which reaches the sediment. By assuming such a flux of Fe-P from the water column into the sediment, the model generates a deep sea burial flux of Fe-P that is consistent with observations, e.g. Fe-P accounts for about 20% of reactive P burial in the deep sea, a sink comparable to that of organic P [*Ruttenberg*, 1993].

2.4. Initial Conditions and Forcing

[16] The present version of the model was run from the reference case of *Heinze et al.* [2006], which is forced by a preindustrial velocity field and adjusted to observed tracer data in the water column (GEOSECS) and the sediment [*Heinze et al.*, 2003]. We set the river input of phosphate to 0.026 Tmol P a^{-1} in agreement with pre-anthropogenic estimates for the input of dissolved reactive P from rivers, which lie in the range of 0.012–0.03 Tmol P a^{-1} [*Wheat et al.*, 1996; *Harrison et al.*, 2005, Figure 1]. In this study, we do not include inputs of particulate P from rivers, though these are known to significantly increase the total input of reactive P to the ocean [*Beusen et al.*, 2005]. This assumption is justified as the model does not give a proper representation of continental margins, where a large fraction of reactive P is buried [*Ruttenberg*, 1993]. Soluble atmospheric P contributes with 0.003 Tmol P a^{-1} to reactive P, representing 10% of the total river input in the model. River fluxes are prescribed as a constant increment to the first wet grid point adjacent to the continent rather than to the entire surface ocean as its was done in previous versions of the model. In addition to the input of terrigenous material (clays) from dust (using the model field of *Andersen et al.* [1998]), we include clays from rivers. *Beusen et al.* [2005] estimated a riverine input of clays to the world coastal

Table 2. Global POC Fluxes in the Model Reference Run and From Observations [*Dunne et al.*, 2007][a]

POC Flux	Global[b]	Deep-Sea
Reference Run		
Export production	9.4	9.05
Deposition on sediments	0.23	0.16
Mineralization in sediments	0.21	0.15
Aerobic mineralization in sediments	0.14	0.12
Anaerobic mineralization in sediments	0.07	0.031
Burial	0.03	0.01
Observations		
Export production	9.6 ± 3.6	6.25 ± 2.55
Deposition on sediments	2.3 ± 0.9	0.31 ± 0.3
Mineralization in sediments	0.7	0.19 ± 0.19
Burial	0.3	0.012 ± 0.02

[a]Units in Gt C yr^{-1}.
[b]Note that in the model coastal zone fluxes are not fully represented. In this context, 'deep sea' refers to the region with water depths >2000 m.

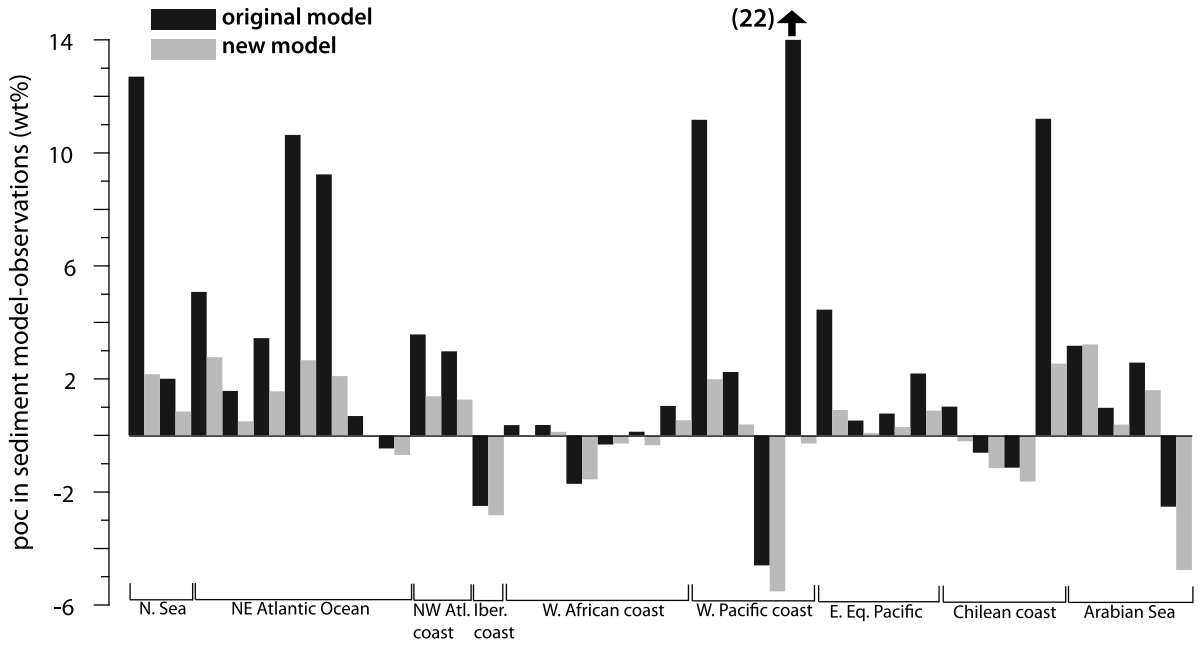

Figure 3. Difference between POC concentrations from the model and observations at the top 1 cm of sediments. Data by *Seiter et al.* [2004], including sites corresponding to 'margin' and 'deep-sea' locations. Black (grey) bars display model-observations in the original (new) version of the model. The arrow in the graph indicates a POC value of 22 wt% at the location.

ocean of 17 Gt a^{-1}. To estimate the input of clays in the model we assume that this flux only reaches the shallowest points in the model, i.e. water depths lower than 500 m, and we scale the total flux by the area of the real coastal ocean, so that in the model we only account for a fraction of the observed input to the coastal zone (i.e., 3.5 Gt a^{-1}; Table 1). There is little information on the flux of riverine clays which is exported from the coastal zone to the open ocean, but recent findings support the existence of an open ocean lithogenic flux of 1 Gt a^{-1} [*Dunne et al.*, 2007]. Based on *Berner* [1982], we prescribe an input of 0.7 Gt a^{-1} of clays over the ocean region with depths greater than 500 m (see Figure 2a).

3. Sediment Phosphorus Data

[17] To compare the model results with the observed distribution of P in surface sediments, a compilation of published data on total P concentrations, P accumulation rates, and P speciation in open ocean sediments was made. Observations on total P in such settings are sparse [*Filippelli*, 1997]. So far, *Baturin* [1988] presented the most extensive geographical distribution of total P concentrations in open ocean sediments, based on a compilation of data from the literature. Here, we include only those data from the study of *Baturin* [1988] for which we were able to retrieve the original source. Reliable P speciation data for open ocean settings are limited to only a handful of studies [*Ruttenberg*, 1993; *Filippelli and Delaney*, 1996; *Poulton and Canfield*, 2006]. Therefore, we also include estimates of P speciation from samples with low temporal resolution near the surface sediment boundary [*Latimer and Filippelli*, 2001; *Schenau et al.*, 2005], and based on the average speciation for sediments older in age [*Latimer et al.*, 2006]. Note that the data on P speciation is restricted to sites with water depths greater than 500 m. A detailed description of the P speciation data, including a list of references, is presented in Table S1 in the auxiliary material[1]; details and references of all other data are shown in Tables S2 and S3.

4. Reference Run Results

[18] In this section, we present the results of the reference run for the new version of the model. We first describe the changes relevant to the cycling of POC and then continue with a description of the vertical distribution of the solid forms of P in the sediment and their spatial distribution in the ocean. Changes in the cycles of $CaCO_3$ and Si are minor relative to the original model results [*Heinze et al.*, 2003], and therefore are not discussed. The model was integrated for 200 ka. At this state, it is very close to equilibrium with global POC export production changing only by 2×10^{-6} Gt C a^{-1}. All model parameters used in this standard run are presented in Table 1. Annual global fluxes of P within the ocean and from the sediment as resulting from the reference run are illustrated in Figure 1. Global bulk numbers relevant to the POC system in the model are summarized in Table 2.

4.1. POC

[19] The modeled pattern of sediment POC (Figure 2b) is in good agreement with global observations of total organic carbon in surface sediments [see *Seiter et al.*, 2004, Figure 1a]. The model reproduces the POC maxima in the eastern equatorial Pacific and along continental margins, and the minima in the center of the subtropical gyres. Because of the

[1]Auxiliary materials are available in the HTML. doi:10.1029/2010GB003827.

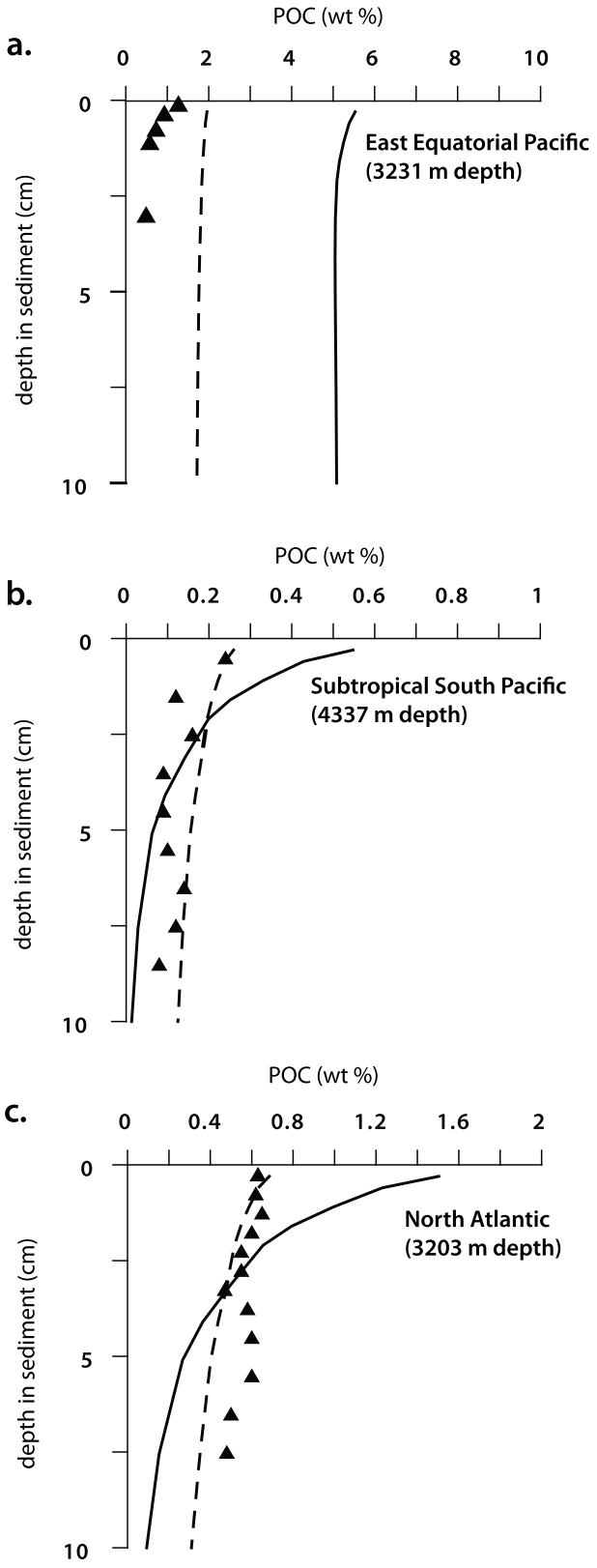

Figure 4. Sediment POC profiles in the original (solid line) and new (dashed line) version of the model for a point in the (a) eastern equatorial Pacific, (93°W, 6°N), (b) subtropical South Pacific, (124°W, 12°S), and (c) North Atlantic, (64°W, 41°N), together with POC observations (triangles) by *Emerson et al.* [1985] and *Emerson and Hedges* [1988].

simplified model bottom topography (Figure 2a), POC concentrations tend to be too large over wide continental shelves such as for example the North Sea and off Patagonia. The difference between the modeled and observed POC concentrations in the top 1 cm of global sediments for the previous and present version of the model is illustrated in Figure 3. Results show that the model-data mismatch is greatly reduced with the new scheme for POC mineralization, especially in high productivity areas in the northeast North Atlantic and along the eastern margins of the subtropical Pacific Ocean, where POC concentrations as high as 10–22 wt% were found previously. On the other hand, the model still underestimates POC concentrations at particular locations along the basins eastern margins and in the Arabian Sea, which in part reflects the inability of the model to properly resolve the productivity in coastal upwelling regimes due to its coarse horizontal resolution. Another limitation in the present formulation is the assumption of fixed uniform rate constants for POC degradation (see section 2.2), while it is known that these vary spatially with water depth [*Middelburg et al.*, 1997] and with the POC flux to the seafloor [*Boudreau*, 1997]. Implementing these empirical relations to specify the value of the rate constants could improve the variability in the modeled POC, but the computational cost is extremely large. Nevertheless, the model already shows that to simulate realistic POC concentrations in areas with high POC deposition, it is necessary to include an anaerobic degradation pathway. A comparison of modeled and observed sediment POC profiles in deep sea sediments is illustrated in Figure 4. Lower POC concentrations near the sediment surface represent an improvement relative to the original model, whereas the agreement between model and data is more ambiguous in the lower part of the profiles, though these differences are relatively small (Figures 4b and 4c). At the shallowest model points, the addition of terrigenous material from rivers alone caused a decrease in the average POC concentrations from 25 to 2.7 wt% (not shown).

[20] The global rate of POC export production predicted by the model (9.4 Gt C a^{-1}) falls in the range of estimates from other general circulation models [*Dunne et al.*, 2007]. However, the modeled POC export production for the deep sea, i.e. the total export production over $z > 2000$ m, lies at the high end of observations (Table 2). Because of the coarse resolution of the model, upwelling velocities in the equatorial zone are too high and induce an overestimation in the POC export production in that region [*Maier-Reimer*, 1993]. Additionally, in particle-only models the productivity in upwelling regions is artificially enhanced by nutrient trapping below the photic zone, which ultimately leads to an overestimation in the nutrient concentrations at intermediate water depths [*Heinze et al.*, 1999]. One way to remedy this deficiency is to include a parameterization to simulate the effect of zooplankton dynamics in removing nutrients from the equatorial zone [*Six and Maier-Reimer*, 1996]. It is also likely that the overprediction in the model tropical export production is related to a considerable numerical diffusivity in the model [*Gnanadesikan et al.*, 2004].

[21] Despite the high rates of POC export production in the model results for the tropical Pacific, POC deposition in this region is underestimated when compared to observations [*Seiter et al.*, 2004]. Overall, the modeled POC depositional flux is significantly lower than the estimate from the data

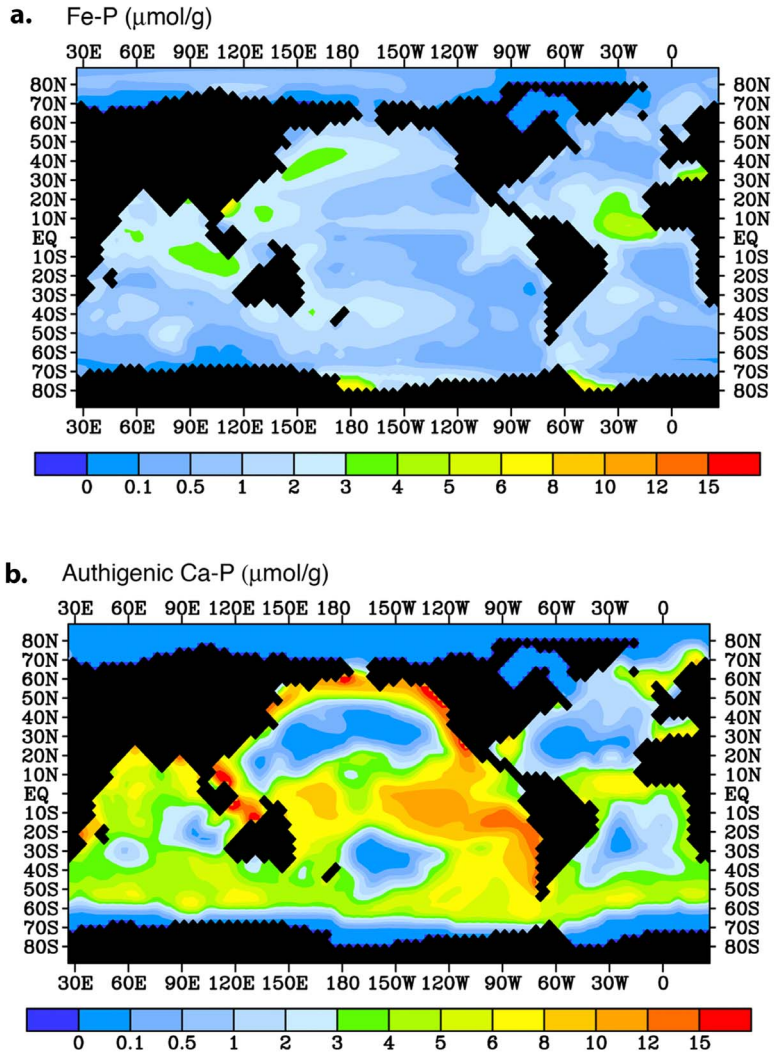

Figure 5. Model reference run results for sediment (a) Fe-P and (b) authigenic Ca-P (both averaged over the entire bioturbated layer). Units in μmol P g^{-1}.

(Table 2). Trends in modeled rates of POC mineralization agree well with observations, with anaerobic mineralization in margin sediments accounting for 70% of the total POC degradation, while in the deep sea this is reversed. Large scale patterns in accumulation rates of POC in the model (Figure 2c) are similar to those from observations [see *Jahnke*, 1996, Figure 4]: high rates are seen in the eastern equatorial Pacific, the Indian Ocean and African high productivity continental margins, while low accumulation rates dominate in the Pacific Ocean subtropical gyres. As for POC concentrations, burial rates over wide continental shelves are overestimated. However, the deep sea burial flux of POC is in good agreement with observations (Table 2).

4.2. Sedimentary P

[22] The distribution and trends of POP in the model closely follow those of POC: the model simulates reasonable POP concentrations in high productivity areas, but underestimates POP along upwelling margins and deep sea oligotrophic regions (not shown). Because of preferential regeneration of P relative to C in anoxic sediments, the model predicts $(C:P)_{org}$ ratios up to [250:1] in the shallowest margin areas and of around [180:1] in sediments below high productivity deep sea regions, like in the eastern equatorial Pacific and northern Indian Ocean, while deep sea oxic sediments show a ratio equal to that adopted for exported POC (e.g.[122:1]). The simulated ratios are consistent with the observation of $(C:P)_{org}$ ratios larger than the Redfield ratio in marine sediments from various ocean basins [*Anderson et al.*, 2001].

[23] The global distribution of sediment Fe-P predicted by the model (averaged over the bioturbated layer) is shown in Figure 5a. Because of the very limited data availability, a global validation of the modeled distribution is not possible. Model results are therefore compared to P speciation data collected from 21 locations over the global ocean (Figure 6 and Table S1). Note that the model-data comparison is based on the model predicted value at the closest grid point to a given observation. This is a valid approximation at deep sea locations, but it becomes critical when referring to points near continental margins, as the model does not have a realistic representation of the bathymetry and intrinsic coastal processes. The model predicts Fe-P maxima in the open

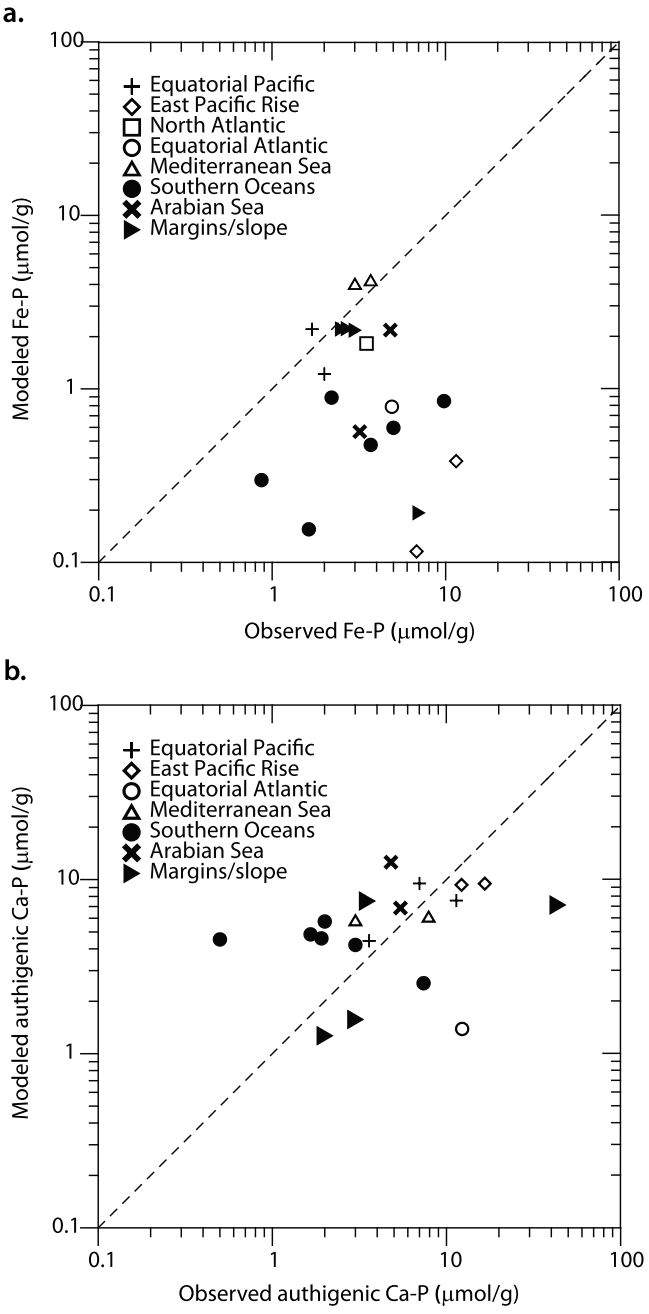

Figure 6. Scatterplot between the observations and model predictions of (a) Fe-P and (b) authigenic Ca-P (in μmol P g^{-1}). Data on P speciation from sediments in the Equatorial Pacific [*Filippelli and Delaney*, 1996; *Murray and Leinen*, 1993]; East Pacific Rise [*Poulton and Canfield*, 2006]; North Atlantic [*Morse*, 1978]; Equatorial Atlantic [*Ruttenberg*, 1993]; Mediterranean Sea [*Slomp et al.*, 2002; *Eijsink et al.*, 2000]; Southern Oceans [*Latimer and Filippelli*, 2001; *Latimer et al.*, 2006]; Arabian Sea [*Schenau et al.*, 2000, 2005]; continental margins and slopes [*Tamburini et al.*, 2003; *Cha etal.*, 2005; *Van der Zee et al.*, 2002; *Slomp et al.*, 1996].

ocean which are associated with Fe-P inputs from atmospheric dust, and average Fe-P concentrations of 0.5–2.0 μmol P g^{-1} globally (Figure 5a). The simulated Fe-P shows a good correspondence with observations in the equatorial Pacific, the Mediterranean Sea, and in general in margin sediments, where model rates of in situ Fe-P precipitation are large; however, the model underestimates Fe-P concentrations in other regions (Figure 6a). The largest discrepancies appear in the metalliferous sediments of the East Pacific Rise, and at a margin location. Overall, the model fails to reproduce the observed Fe-P concentrations over the Southern Oceans. Data from this region must be taken with caution, as some of the estimates are either extracted from data with a very coarse resolution close to the sediment-water interface [*Latimer and Filippelli*, 2001], or calculated using the average P speciation from sediments Pleistocene in age [*Latimer et al.*, 2006]. Samples from anoxic sediments could present problems in the estimate for the Fe-P fraction if exposure to oxygen after core recovery occurred [*Kraal et al.*, 2009]. Vertical sediment profiles of Fe-P in the model are shown for two different settings in Figure 7, together with the corresponding profiles of dissolved pore water PO_4. While Fe-P is almost completely reduced at depth in margin sediments (Figure 7a), Fe-P concentrations vary little with depth at deep sea locations (Figure 7c), largely because of the high oxygen content of pelagic sediments. The range and shape of the model pore water PO_4 profiles (Figures 7b and 7d) are consistent with observations for deep sea and margin environments [*Morse*, 1978; *Slomp et al.*, 1996; *Hensen et al.*, 1998, 2000].

[24] Figure 5b presents the simulated pattern of sediment authigenic Ca-P (averaged over the bioturbated layer). The modeled authigenic Ca-P shows maximum concentrations (8–15 μmol P g^{-1}) off the South and North American western coasts and extending over the eastern equatorial Pacific region up to 165°W. The prediction of Ca-P maxima off western continental margins is consistent with the knowledge of highly rich P deposits being formed off the coasts of Peru and Baja California [*Froelich et al.*, 1988; *Ingall and Jahnke*, 1994]. For the rest of the oceans, the model shows disseminated Ca-P concentrations in the range of 3–6 μmol P g^{-1}, with minima in oligotrophic regions of the basin subtropical gyres. A comparison between model and observations indicates good agreement, specially in the tropical Pacific Ocean, though the model has difficulty to reproduce the variability over the Southern Oceans (Figure 6b). Simulated high concentrations over the equatorial Atlantic and the Mediterranean Sea reflect the influence of authigenic Ca-P deposition from Saharan dust, however, the model estimate falls below the observed value in the equatorial Atlantic around 5°S (Figure 6b). A possible explanation is that at this site a background P phase is present in the form of, for example, P associated with clays [*Ruttenberg and Berner*, 1993].

[25] The distribution of total (reactive and detrital) P in the model is presented and compared to observations in Figure 8. The model is able to reproduce most of the trends seen in the data: high P concentrations are observed close to continental margins, in the eastern Indian Ocean, and over the central-eastern tropical Pacific, whereas low P concentrations are typical of the Atlantic Ocean. Quantitatively, simulated P concentrations are lower than observations in the central tropical Pacific and the Atlantic Ocean. The discrepancy relates in part to the fact that the data includes P observations from East Pacific Rise sediments (i.e. six locations between 10°–20°S, 100°–120°W from *Berner* [1973]; *Froelich et al.* [1977]; *Poulton and Canfield* [2006]), and subtropical red clay provinces enriched in P [*Baturin*, 1988]).

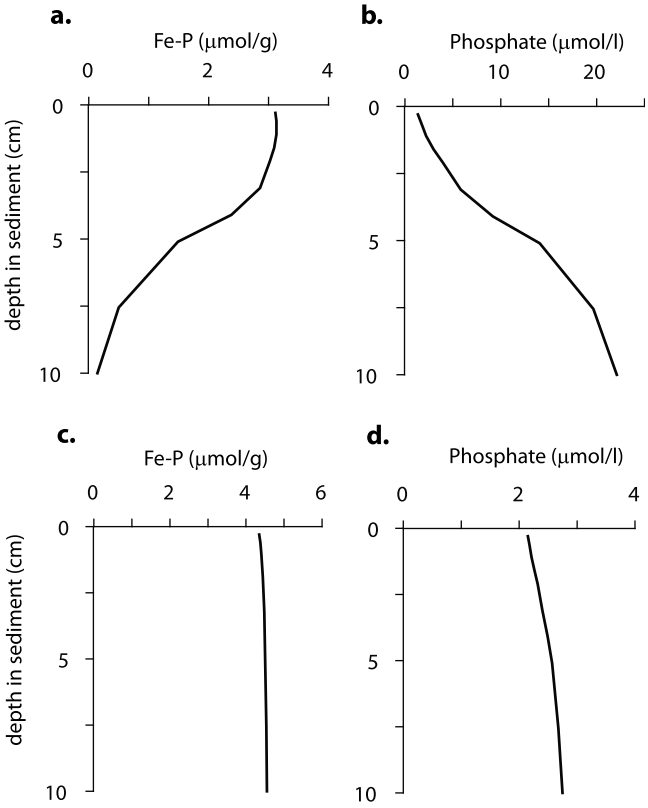

Figure 7. Profiles of sediment Fe-P and pore water phosphate at a location in (a, b) margin sediments (0°E, 55°N; 694 m water depth) and (c, d) deep sea sediments (23°W, 3°S; 4580 m water depth), in the model reference run.

The widespread low P concentrations over the Atlantic basin in the model contrast with observations that suggest a minimum of P along the Mid-Atlantic Ridge area and higher P concentrations toward margins due to the large influence of continental river runoff in this basin [see *Baturin*, 1988, Figure 3]. The results here show that detrital inputs of P from Saharan dust play a key role in generating relatively high sediment P concentrations in the tropical Atlantic, the western tropical North Atlantic sector, and in the eastern tropical Pacific along 10°N. In general, the model estimates of detrital apatite (e.g. 1–6 μmol P gr^{-1}) are consistent with local observations (not shown).

[26] The pattern of total reactive P burial (POP + Ca-P + Fe-P) in the model reflects high burial rates in the form of POP and Ca-P over depositional margin areas and in the eastern equatorial Pacific, whereas relatively high burial rates in the deep sea are mostly due to Ca-P (Figure 8c). Simulated rates of Fe-P burial are mostly significant over the tropical Atlantic Ocean. The modeled rate of total reactive P burial for the deep sea equals 0.023 Tmol P a^{-1}, which is in agreement with low end estimates from observations [*Ruttenberg*, 1993; *Delaney*, 1998]. In addition, the global fractionation of reactive P burial in the model (60% as Ca-P, 22% as POP and 18% as Fe-P) is consistent with that estimated for the deep sea [*Ruttenberg*, 1993; *Filippelli and Delaney*, 1996] and continental slope sediments [*Slomp et al.*, 1996]. Comparison of the total P accumulation rates in the model with local observations shows that model estimates tend to be lower than observations in deep sea oligotrophic regions (see data in Table S3). In particular, the model underestimates rates of total P burial in the central tropical/subtropical Pacific Ocean and at locations in the South Atlantic and South Indian Ocean. These deficiencies are possibly related to the total sedimentation rates in the model, and to an underestimation of the simulated total P concentrations at these locations.

5. Sensitivity Experiments

[27] In this section, we investigate the response of the model to an increase in the riverine supply of reactive P relative to the standard case. We specifically focus on the feedback loop between P availability, primary production, bottom water anoxia and P regeneration from sediments [*Van Cappellen and Ingall*, 1994]. In addition to the reference run ('control'), we consider two control runs with different degrees of preferential P release from anaerobic degradation of organic matter, i.e. a run with no preferential P regeneration (α = 1; 'control$_1$') and a run with larger preferential P regeneration (α = 3; 'control$_3$'). The experiments were run over 200 ka to capture the timescale of the adjustment to a new equilibrium (determined by the model P residence time, of about 120 ka). The various runs are listed in Table 3 along with the global fluxes of POC export production and benthic P regeneration at the new state.

[28] The benthic P regeneration flux in the model is calculated from the difference between the depositional flux of P and the total P burial rate. The spatial distribution of this flux is similar to the pattern of POC deposition, reflecting the importance of sediment POC mineralization for P regeneration. The global rate of P regeneration in the model reference run is 0.13 Tmol P a^{-1}, and 0.09 Tmol P a^{-1} if only the deep sea area is considered. Estimates of the global benthic P flux based on pore water data yield values between 0.41 Tmol P a^{-1} for deep sea and continental rise sediments [*Colman and Holland*, 2000], and 0.32 Tmol P a^{-1} for water depths >1000 m [*Hensen et al.*, 1998]. A low value for the benthic P flux as calculated here reflects the coarse resolution of the model near margins as well as an underestimation of the POC depositional flux at deep sea locations. In addition, the model excludes lateral export of terrigenous POC from coastal areas to the open ocean [*Hensen et al.*, 2000]. Local rates of benthic P release in the model are highest over margins, reaching values of 3 to 10 mmol P m^{-2} a^{-1}. These compare well to the lower range of benthic P fluxes observed in continental shelf locations, i.e. 2–20 mmol P m^{-2} a^{-1} [*Ingall and Jahnke*, 1994; *Cha et al.*, 2005; *Hensen et al.*, 2000]. Increasing the degree of preferential P regeneration in the model control runs leads to a relatively minor increase in the global benthic P flux, i.e. from 0.12 to 0.14 Tmol P a^{-1} when α varies from 1 to 3 (Table 3).

[29] We now analyze the response of the model to a doubling in the input of dissolved P from rivers relative to the control runs with different values of the parameter α. The simulations show an increase in the global rate of POC export production of 50–55% (Figure 9a). In particular, the results show that including a mechanism for preferential P regeneration in the sediment increases the global export production rate by about 1 Gt C a^{-1} (compare, for example, the amplification of the initial difference in export production between runs dbl$_1$ and dbl$_3$). Because of increased respiration

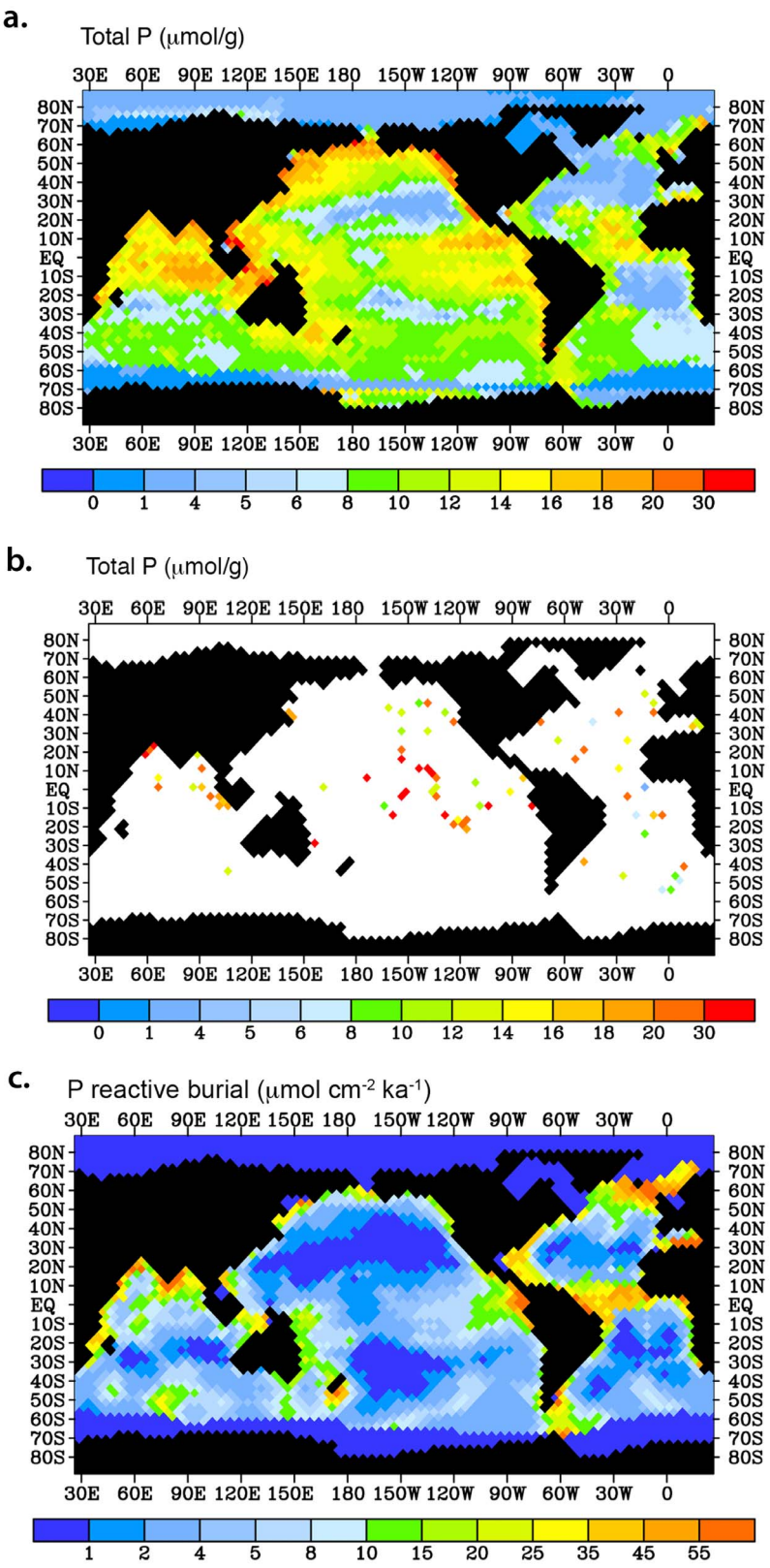

Figure 8. Total P concentrations (μmol P g^{-1}) in surface sediments (a) in the model reference run (averaged over the entire bioturbated layer) and (b) from observations collected from the literature (Table S2). (c) Total reactive P accumulation rates (μmol cm^{-2} ka^{-1}).

Table 3. List of Model Sensitivity Experiments, Together With the Associated Global Rates of POC Export Production (Gt C a^{-1}) and Benthic P Flux (Tmol P a^{-1})[a]

Run	Description	POC Export	Benthic P Flux
Control	reference run (α = 2)	9.4	0.13
$Control_1$	as reference, but with α = 1	8.5	0.12
$Control_3$	as reference, but with α = 3	9.8	0.14
dbl_1	river P input × 2, α = 1	12.9	0.16
dbl_2	river P input × 2, α = 2	14.2	0.19
dbl_3	river P input × 2, α = 3	15.1	0.2
$dbl_{2,Ca}$	as dbl_2, but with less Ca-P formation (2 × C_a)	16.6	0.23
$dbl_{3,Ca}$	as dbl_3, but with less Ca-P formation (2 × C_a)	17.9	0.25
$dbl+_2$	river P input × 2.5, α = 2	16.1	0.21
$dbl+_{2,Ca}$	as $dbl+_2$, but with less Ca-P formation (2 × C_a)	19	0.26
$dbl_{2,Ca,FeP}$	as $dbl_{2,Ca}$but with no sediment Fe-P	17.2	0.24

[a]Values of the parameter α represent the degree of preferential regeneration of P relative to C from organic matter under anoxic sediment conditions.

in the water column, the mean oxygen concentration at 2000 m depth shows a significant drop to values below 100 μM in all cases of preferential P regeneration (Figure 9b). Still, for these forcing conditions the feedback from preferential P release on the final response to a doubling in river P input is moderate. Ultimately, the boost in primary productivity leads to an increase in the burial of all forms of reactive P, with a 75% increase in authigenic Ca-P burial. This implies that in these experiments the magnitude of the P regeneration flux is limited by a large increase in authigenic Ca-P concentrations at deep sea locations.

[30] Observations for several recent low oxygen marine systems [*Schenau et al.*, 2000; *Slomp et al.*, 2002; *Tamburini et al.*, 2003] and for Cretaceous sediments during OAEs [*Mort et al.*, 2007] suggest, however, that authigenic Ca-P formation can be limited in deep sea sediments. The suggested mechanism for less effective authigenic Ca-P formation in anoxic deep sea settings is that P is released very close to the sediment-water interface, from where it can be quickly lost to the overlying water column in the absence of Fe-oxides. In addition, the rise in alkalinity associated with increased sulfate reduction may hinder authigenic apatite formation [*Tribovillard et al.*, 2010]. To constrain the rate of P retention by authigenic Ca-P precipitation in sediments, we consider simulations with a lower rate of Ca-P precipitation by doubling the value of the equilibrium constant C_a with respect to the standard case. Note that such a choice for C_a is not arbitrary, as it falls in the range of values expected for normal T and pH conditions in the ocean [*Van Cappellen and Berner*, 1988]. In this case, a doubling in the input of P from rivers results in a pattern of authigenic Ca-P in the sediment still similar to the reference case, with a 25% increase in the Ca-P burial rate. Simulations with a lower rate of authigenic

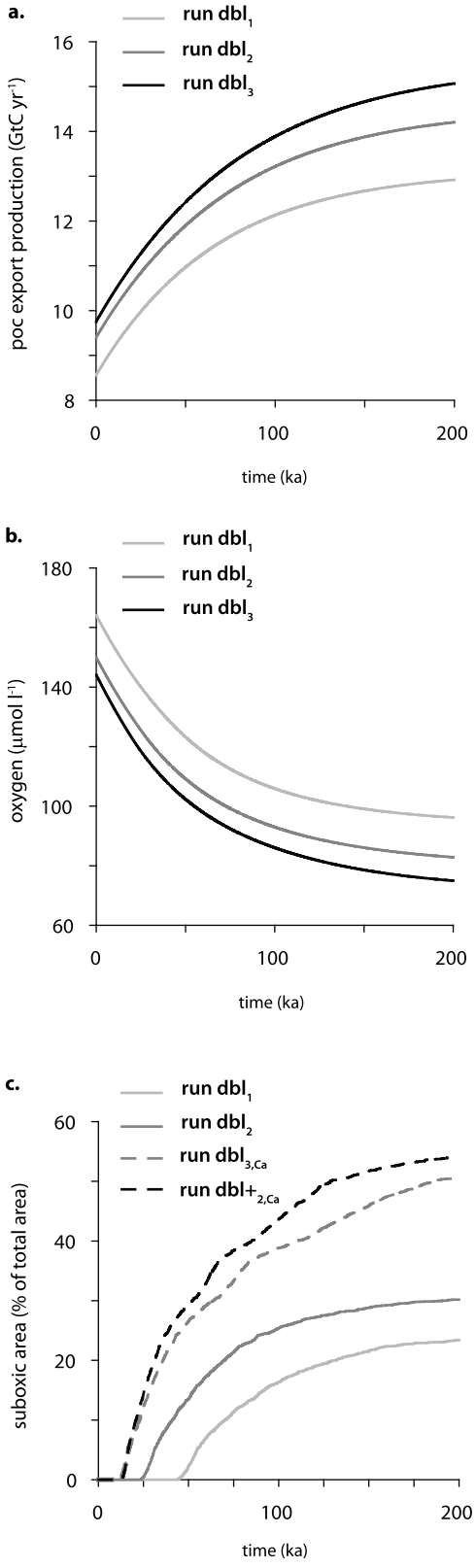

Figure 9. Response of the modeled (a) global rate of POC export production and (b) mean oxygen concentration at 2000 m depth to a doubling in the input of P from rivers, with different degrees of preferential P regeneration. (c) Change in the modeled suboxic area (O_2 < 25 μM) at 2000 m depth due to a doubling in the input of P from rivers, with standard conditions (dark gray line, dbl_2), large benthic P flux (dashed gray line, $dbl_{3,Ca}$), and no preferential P regeneration (light grey line, dbl_1); and for 2.5 times the standard rate of riverine input of P and reduced authigenic Ca-P formation (dashed black line, $dbl+_{2,Ca}$).

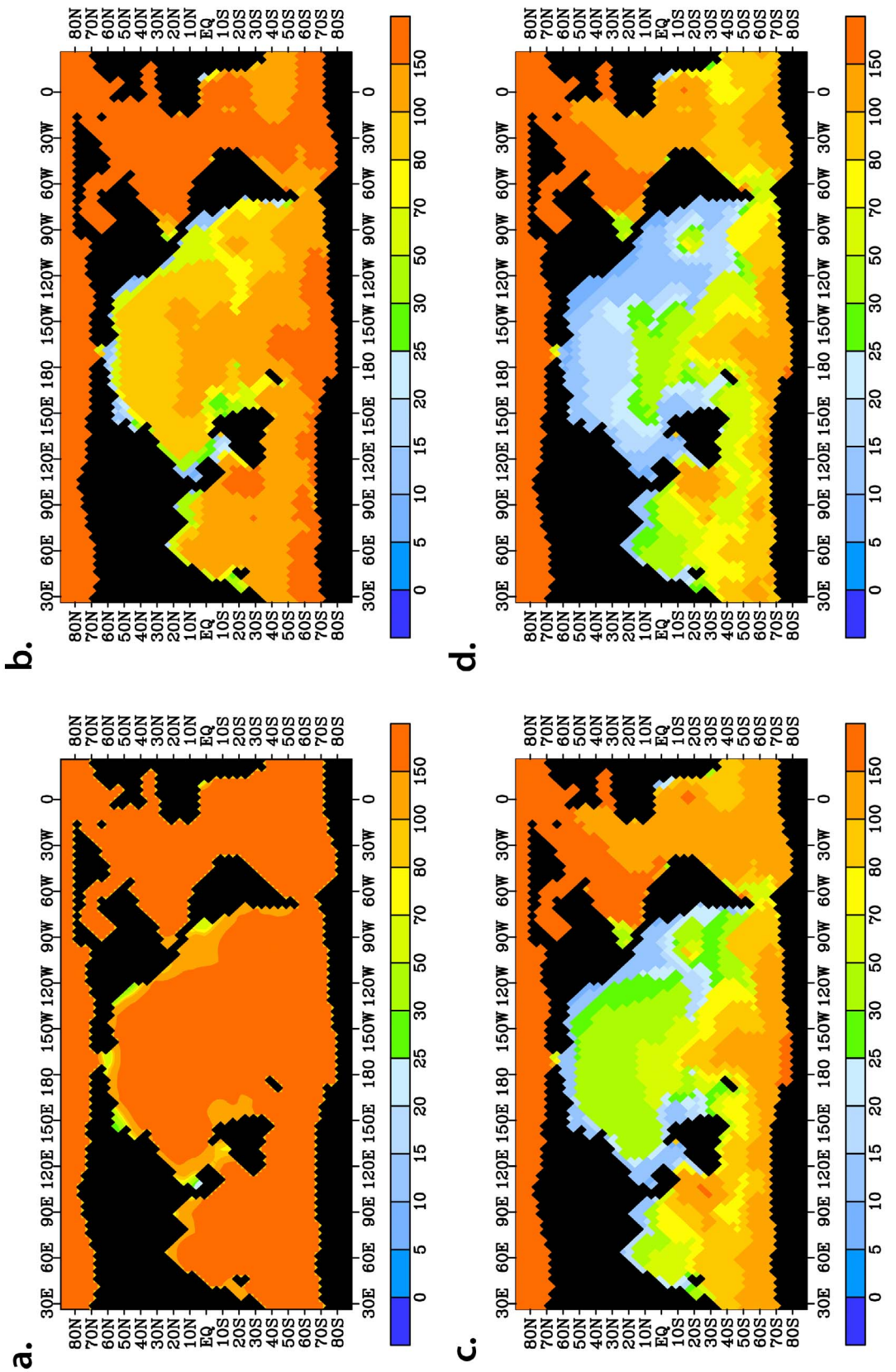

Figure 10. Bottom water oxygen concentration (μM) in the (a) model reference run and for the experiments with (b) a doubling in the input of P from rivers and standard conditions (dbl_2), (c) a doubling in the input of P from rivers and large benthic P flux ($dbl_{3,Ca}$), and (d) 2.5 times the standard input of P from rivers and reduced authigenic Ca-P formation ($dbl^{+}_{2,Ca}$).

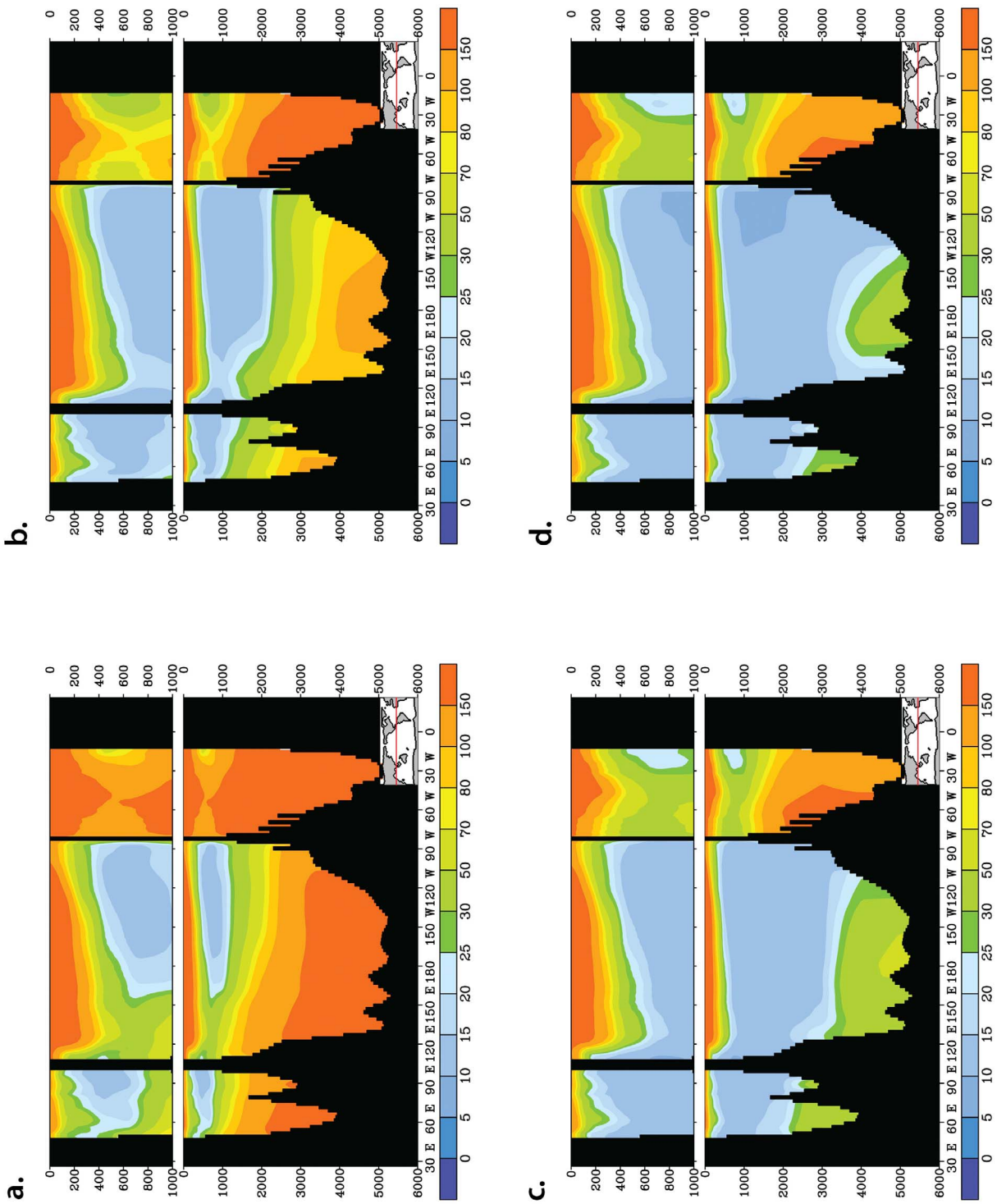

Figure 11. Oxygen zonal section along 11°N. (a) Model reference run. Model results for (b) a doubling in the input of P from rivers and standard conditions (dbl_2), (c) a doubling in the input of P from rivers and large benthic P flux ($dbl_{3,Ca}$), and (d) 2.5 times the standard input of P from rivers and reduced authigenic Ca-P formation ($dbl+_{2,Ca}$). Units in μM.

Ca-P formation relative to the standard case show a significant increase in the benthic P flux if preferential P regeneration is also taken into account (Table 3, runs $dbl_{2,Ca}$ and $dbl_{3,Ca}$). Because of enhanced release of P from sediments, the final response in global POC export production is amplified by 2.4–2.8 GtC a^{-1} and mean deep water oxygen concentrations are about 60 μM (not shown).

[31] The patterns of bottom water oxygen illustrate in what ocean areas the coupling between primary productivity, bottom water oxygen, and benthic P release is strong. The experiments with a doubling in the riverine input of P show an increase (relative to the reference run) in bottom water suboxia (defined here as $O_2 < 25$ μM) along the continental margins of the Pacific basin, both at tropical latitudes and at midlatitude locations with high rates of POC deposition (Figures 10a and 10b). This pattern is amplified and extends into the deep sea and North Indian Ocean, in the case of a larger benthic P flux, for example if maximum preferential P regeneration and a reduced Ca-P sink are enabled (Figure 10c). So, outside high depositional margins, the eastern and western tropical Pacific, where $(C:P)_{org}$ ratios and Ca-P concentrations are normally high, appear as deep sea areas susceptible to develop a strong feedback between sedimentary P recycling and deep water oxygen. This contrasts with the situation in the Atlantic Ocean, where high rates of oceanic ventilation induce well oxygenated waters and only in very localized high productivity areas bottom waters become suboxic.

[32] To test the effect of a further increase in the input of P from rivers, simulations with an input of P that is 2.5 times the preindustrial rate were run. The results indicate a maximum value for the benthic P flux (Table 3, $dbl+_{2,Ca}$). Bottom water suboxia extends over the southeastern Pacific sector and in the tropical Pacific, while the advective effect of ocean circulation spreads suboxia into the northern Pacific basin (Figure 10d), which results in a suboxic pattern that covers 30% of the total ocean area. Although a larger input of reactive P is not unreasonable given the range of uncertainty in current estimates of P input from rivers [*Delaney*, 1998], the simulations indicate that to generate such a large-scale pattern of bottom water suboxia, large recycling of P from sediments is also needed.

[33] Modeled changes in deep water oxygenation due to increases in the input of P from rivers are associated with the behavior of the tropical oxygen minimum zones (OMZ). An oxygen zonal section along 11°N illustrates that for the reference run, an OMZ is present in the eastern and central Pacific Ocean between 400–1000 m and in the eastern Indian Ocean around 500 m (Figure 11a). A comparison to observed oxygen meridional sections in the east and west Pacific (not shown), indicates that the model overestimates the extension of the OMZ in the central-western basin and predicts a deeper minimum there, which is a model deficiency related to nutrient trapping in tropical upwelling areas [*Six and Maier-Reimer*, 1996]; on the other hand, the model underestimates the magnitude of the oxygen minimum in the eastern North Pacific. The experiments with a doubling in P river inputs show an expansion of the OMZ down to 2000 m in the eastern Pacific and below 1000 m in the tropical Indian Ocean (Figure 11b). The OMZ reaches to depths below 3000 m in the eastern equatorial Pacific for an increase in the benthic P flux (Figure 11c), and to abyssal depths in case of maximum benthic P flux (Figure 11d). In general, the results show that an initial expansion of the OMZ in the eastern Pacific and Indian Ocean could be potentially reinforced by the release of P from sediments of these high productivity areas. An estimate of the modeled total suboxic area at 2000 m depth indicates that when the input of P from rivers is doubled, including a mechanism for P regeneration in the sediment accelerates the initiation of the suboxic expansion from 45 ka (Figure 9c, dbl_1) to 12 ka (Figure 9c, $dbl_{3,Ca}$). For a further increase in the riverine supply of P and large P recycling, the expansion of suboxia starts after 13 ka (Figure 9c, $dbl+_{2,Ca}$).

[34] Despite the change in sediment redox conditions toward anoxia, all the simulations present an increase in the rate of Fe-P burial. This is because the increase in the rates of P sorption (as pore water phosphate increases) in deep sea locations overcomes the effect of reductive dissolution of Fe-oxides and release of Fe-P, resulting in average sediment Fe-P concentrations of the same order as those in the reference run. To evaluate the possible maximum effect of redox dependent Fe-P burial on the modeled benthic P flux, we force complete dissolution of Fe-P in one of the experiments with a doubling in river P input. The results show a relative increase in POC export production of 0.6 Gt C a^{-1} and in the P regeneration flux of 0.01 Tmol P a^{-1} (Table 3, $dbl_{2,Ca,FeP}$). The magnitude of these changes suggest that in reality reductive dissolution of Fe-P may have a relatively minor contribution to the feedback mechanism from redox-dependent P regeneration on a global scale.

6. Summary and Outlook

[35] In this study, sediment P dynamics were implemented for the first time in a biogeochemical ocean general circulation model, which was originally developed to describe the oceanic carbon and silicon cycles. This modeling approach allows long-term integrations on the order of 200 ka. However, the model does not resolve the coastal zone, which implies that organic C and P burial fluxes predicted by the model can only be compared to observations for the deep sea ($z > 2000$ m). In agreement with observations, the results for preindustrial conditions show that authigenic Ca-P is the main sink of reactive P in the open ocean (60% of total reactive P burial), followed by the organic P (22%) and Fe-P (18%) sink. The sensitivity of the model to a doubling in the supply of dissolved P from rivers shows that enhanced recycling of reactive P from sediments amplifies the long-term global response in primary productivity and oxygen depletion along continental margins and in the bulk of the tropical OMZs. The feedback between primary productivity, bottom water suboxia, and preferential P regeneration in the open ocean involves the eastern and western tropical Pacific Ocean, and the southeastern Pacific sector, which are regions with normally high $(C:P)_{org}$ ratios in the sediment. The strength of this feedback, however, is very sensitive to the rate of authigenic Ca-P burial in the deep sea. Nonetheless, the results suggest that preferential regeneration of P from anoxic POC degradation accelerates the expansion of ocean suboxia below 1000 m depths.

[36] The description of the sedimentary P cycle and redox-dependent P regeneration presented here is limited by several model simplifications. Model estimates of sediment P could be improved in the future by the regionally varying

addition of terrigenous inputs of particulate P from rivers [*Beusen et al.*, 2005] into the open ocean. In particular, this could improve the results for the Atlantic Ocean, where the continental influence upon sedimentation is the strongest [*Baturin*, 1988]. Still, for a meaningful model-data comparison more observations on sediment P are needed for deep sea settings, especially at mid and high latitudes in the Southern Hemisphere. Another limitation of the present model is an underestimation of the POC flux to the seafloor in deep sea regions. Including mineral ballast effects in the formulation for the vertical transport of POC in the water column could potentially improve the results [*Dunne et al.*, 2007]. This would eventually increase the model benthic P flux in the deep sea, which is currently lower than estimates from observations and modeling [*Wallmann*, 2003]. However, to properly simulate the magnitude of the P regeneration flux on a global scale, further constraints on the mechanism of redox dependent Ca-P formation and burial in deep sea sediments are needed. The results here suggest that a better understanding of the relationship between POC burial and authigenic Ca-P formation in tropical/subtropical Pacific sediments is relevant for long-term variations in ocean oxygenation.

[37] Our idealized experiments show that increasing 2 to 2.5 times the preindustrial input of P from rivers, together with large sediment P recycling, leads to large-scale bottom water suboxia on geological timescales. The essential role played by sediment P regeneration in expanding suboxia is similar to the findings for Cretaceous OAEs [*Handoh and Lenton*, 2003; *Tsandev and Slomp*, 2009]. However, while in the model of *Tsandev and Slomp* [2009] a decrease in ocean circulation is an additional necessary condition to sustain deep ocean anoxia, in the simulations here the circulation does not change. We find that reductive dissolution of Fe-P in the deep sea has a minor impact on the feedback between long-term productivity and deep water anoxia. *Handoh and Lenton* [2003] also identified that the feedback from Fe-P burial is not essential to sustain the low frequency oxic-anoxic oscillations in their model whereas that from organic P burial is. We note that in the present approach, the timescale of adjustment of the coupled C, P and O_2 cycles to perturbation is linked to the residence time of P in the model which is about 120 ka, reflecting the lack of the coastal P sink. In addition, because the dynamics of the coastal zone are not explicitly represented, the cycling of reactive P in the open ocean in response to increases in P river inputs might be overestimated [*Slomp and Van Cappellen*, 2007].

[38] There is now evidence that oxygen depletion and vertical expansion of natural suboxic areas is occurring in the tropical Atlantic and Pacific Ocean in response to global warming [*Stramma et al.*, 2008]. Simulations with fully coupled GCMs for future CO_2 scenarios predict oxygen depletion and vertical expansion of OMZs to continue over the next 1000 to 10000 years, and these changes are significantly amplified if a weakening in the meridional overturning circulation is also considered [*Shaffer et al.*, 2009]. Our study suggests that on these spatial and temporal scales preferential P regeneration from sediments provides an additional positive feedback to promote the expansion of oxygen depletion in the deep sea which may eventually cause ocean suboxic conditions to persist longer in the basin. The amplitude and timescale of this feedback however, will depend on the interaction with other positive feedbacks in the climate system, including changes in river inputs due to increased weathering in a warmer climate and changes in ocean biogeochemistry [*Oschlies et al.*, 2008]. In this context, Earth System Models should include preferential P regeneration from sediments when assessing future climate predictions on timescales of 10 to 100 ka AD.

[39] **Acknowledgments.** This is publication DW-2011-1010 of the Darwin Center for Biogeosciences. We also acknowledge funding from the Netherlands Organisation for Scientific Research (NWO-Vidi grant to C. P. Slomp) and from Utrecht University (High Potential grant). This is publication A 340 from the Bjerknes Centre for Climate Research. We thank Arne Winguth (University of Texas at Arlington) for the LSG velocity field. We thank an anonymous reviewer for insightful comments that greatly improved the manuscript.

References

Andersen, K. K., A. Armengaud, and C. Genthon (1998), Atmospheric dust under glacial and interglacial conditions, *Geophys. Res. Lett.*, *25*, 2281–2284.

Anderson, L. A., and J. L. Sarmiento (1994), Redfield ratios of remineralization determined by nutrient data analysis, *Global Biogeochem. Cycles*, *8*, 65–80.

Anderson, L. D., M. L. Delaney, and K. L. Faul (2001), Carbon to phosphorus ratios in sediments: Implications for nutrient cycling, *Global Biogeochem. Cycles*, *15*, 65–79.

Atlas, E., and R. M. Pytkowicz (1977), Solubility behaviour of apatites in seawater, *Limnol. Oceanogr.*, *2*, 290–300.

Baker, A., T. D. Jickells, and K. L. Linge (2006), Trends in solubility of iron, aluminium, manganese and phosphorus in aerosol collected over the Atlantic Ocean, *Mar. Chem.*, *98*, 43–58.

Baturin, G. N. (1988), Disseminated phosphorus in oceanic sediments—A review, *Mar. Geol.*, *84*, 95–104.

Benitez-Nelson, C. R. (2000), The biogeochemical cycling of phosphorus in marine systems, *Earth Sci. Rev.*, *51*, 109–135.

Berner, R. A. (1973), Phosphate removal from sea water by adsorption on volcanogenic ferric oxides, *Earth Planet. Sci. Lett.*, *18*, 77–86.

Berner, R. A. (1982), Burial of organic carbon and pyrite sulfur in the modern ocean: Its geochemical and environmental significance, *Am. J. Sci.*, *282*, 451–473.

Beusen, A. H. W., A. L. M. Dekkers, A. F. Bouwman, W. Ludwig, and J. Harrison (2005), Estimation of global river transport of sediments and associated particulate C, N, and P, *Global Biogeochem. Cycles*, *19*, GB4S05, doi:10.1029/2005GB002453.

Boudreau, B. P. (Ed.) (1997), *Diagenetic Models and Their Implementation*, 414 pp., Springer, Berlin.

Cha, H. J., C. B. Lee, B. S. Kim, M. S. Choi, and K. C. Ruttenberg (2005), Early diagenetic redistribution and burial of phosphorus in the sediments of the southwestern East Sea (Japan Sea), *Mar. Geol.*, *216*, 127–143.

Colman, A. S., and H. D. Holland (2000), The global diagenetic flux of phosphorus from marine sediments to the oceans: Redox sensitivity and the control of atmospheric oxygen levels, in *Marine Authigenesis: From Global to Microbiological*, *Spec. Publ. SEPM Soc. Sediment. Geol.*, *66*, 53–75.

Delaney, M. L. (1998), Phosphorus accumulation in marine sediments and the oceanic phosphorus cycle, *Global Biogeochem. Cycles*, *12*, 563–572.

Dunne, J. P., J. L. Sarmiento, and A. Gnanadesikan (2007), A synthesis of global particle export from the surface ocean and cycling through the ocean interior and on the seafloor, *Global Biogeochem. Cycles*, *21*, GB4006, doi:10.1029/2006GB002907.

Eijsink, L. M., M. D. Krom, and B. Herut (2000), Speciation and burial flux of phosphorus in the surface sediments of the eastern Mediterranean, *Am. J. Sci.*, *300*, 483–503.

Emerson, S., and J. I. Hedges (1988), Processes controlling the organic carbon content of open ocean sediments, *Paleoceanography*, *3*, 621–634.

Emerson, S., K. Fischer, C. Reimers, and D. Heggie (1985), Organic carbon dynamics and preservation in deep sea sediments, *Deep Sea. Res.*, *32*, 1–21.

Filippelli, G. M. (1997), Controls on phosphorus concentration and accumulation in oceanic sediments, *Mar. Geol.*, *139*, 231–240.

Filippelli, G. M., and M. L. Delaney (1996), Phosphorus geochemistry of equatorial Pacific sediments, *Geochim. Cosmochim. Acta*, *60*, 1479–1495.

Froelich, P. N., M. L. Bender, and G. R. Heath (1977), Phosphorus accumulation rates in metalliferous sediments on the East Pacific Rise, *Earth Planet. Sci. Lett.*, *34*, 351–359.

Froelich, P. N., et al. (1988), Early diagenesis of organic matter in Peru continental margin sediments: Phosphorite precipitation, *Mar. Geol.*, *80*, 309–343.

Gislason, S. R., et al. (2009), Direct evidence of the feedback between climate and weathering, *Earth Planet. Sci. Lett*, *227*, 213–222.

Gnanadesikan, A., J. P. Dunne, R. M. Key, K. Matsumoto, J. L. Sarmiento, R. D. Slater, and P. S. Swathi (2004), Oceanic ventilation and biogeochemical cycling: Understanding the physical mechanisms that produce realistic distributions of tracers and productivity, *Global Biogeochem. Cycles*, *18*, GB4010, doi:10.1029/2003GB002097.

Graham, W. F., and R. A. Duce (1979), Atmospheric pathways of the phosphorus cycle, *Geochim. Cosmochim. Acta*, *43*, 1195–1208.

Gypens, N., C. Lancelot, and K. S. Soetaert (2008), Simple parameterisations for describing N and P diagenetic processes: Application in the North Sea, *Prog. Oceanogr.*, *76*, 89–110.

Handoh, I. C., and T. M. Lenton (2003), Periodic mid-Cretaceous oceanic anoxic events linked by oscillations of the phosphorus and oxygen biogeochemical cycles, *Global Biogeochem. Cycles*, *17*(4), 1092, doi:10.1029/2003GB002039.

Harrison, J. S., S. P. Seitzinger, A. F. Bouwman, N. F. Caraco, A. H. W. Beusen, and C. J. Vörösmarty (2005), Dissolved inorganic phosphorus export to the coastal zone: Results from a spatially explicit global model, *Global Biogeochem. Cycles*, *19*, GB4S03, doi:10.1029/2004GB002357.

Heinze, C., E. Maier-Reimer, A. M. E. Winguth, and D. Archer (1999), A global oceanic sediment model for long-term climate studies, *Global Biogeochem. Cycles*, *13*, 221–250.

Heinze, C., A. Hupe, E. Maier-Reimer, N. Dittert, and O. Ragueneau (2003), Sensitivity of the marine Si cycle for biogeochemical parameter variations, *Global Biogeochem. Cycles*, *17*(3), 1086, doi:10.1029/2002GB001943.

Heinze, C., M. Gehlen, and C. Land (2006), On the potential of ^{230} Th, ^{231} Pa, and ^{10} Be for marine rain ratio determinations, *Global Biogeochem. Cycles*, *20*, GB2018, doi:10.1029/2005GB002595.

Hensen, C., H. Landenberger, M. Zabel, and H. D. Schulz (1998), Quantification of diffusive benthic fluxes of nitrate, phosphate and silicate in the southern Atlantic Ocean, *Global Biogeochem. Cycles*, *12*, 193–210.

Hensen, C., M. Zabel, and H. D. Schulz (2000), A comparison of benthic nutrient fluxes from deep sea sediments off Namibia and Argentina, *Deep Sea Res., Part II*, *47*, 2029–2050.

Hofmann, M., and H. J. Schellnhuber (2009), Ocean acidification affects marine carbon pump and triggers extended marine oxygen holes, *Proc. Natl. Acad. Sci. U. S. A.*, *106*(9), 3017–3022.

Ingall, E., and R. Jahnke (1994), Evidence for enhanced phosphorus regeneration from marine sediments overlain by oxygen depleted waters, *Geochim. Cosmochim. Acta*, *58*, 2571–2575.

Jahnke, R. A. (1996), The global ocean flux of particulate organic carbon: Areal distribution and magnitude, *Global Biogeochem. Cycles*, *10*, 71–88.

Kraal, P., C. P. Slomp, A. Forster, M. M. M. Kuypers, and A. Sluijs (2009), Pyrite oxidation during sample storage determines phosphorus fractionation in carbonate-poor anoxic sediments, *Geochim. Cosmochim. Acta*, *73*, 3277–3290.

Krom, M. D., and R. A. Berner (1980), Adsorption of phosphate in anoxic marine sediments, *Limnol. Oceanogr.*, *25*, 797–806.

Latimer, J. C., and G. M. Filippelli (2001), Terrigenous input and paleoproductivity in the Southern Ocean, *Paleoceanography*, *23*, 627–643.

Latimer, J. C., G. M. Filippelli, I. Hendy, and D. R. Newkirk (2006), Opal associated particulate phosphorus: Implications for the marine P cycle, *Geochim. Cosmochim. Acta*, *70*, 3843–3854.

Mahowald, N., et al. (2008), Global distribution of atmospheric phosphorus sources, concentrations and deposition rates, and anthropogenic impacts, *Global Biogeochem. Cycles*, *22*, GB4026, doi:10.1029/2008GB003240.

Maier-Reimer, E. (1993), Geochemical cycles in an ocean general circulation model: Preindustrial tracer distributions, *Global Biogeochem. Cycles*, *7*, 645–677.

Maier-Reimer, E., U. Mikolajewicz, and K. Hasselmann (1993), Mean circulation of the Hamburg LSG OGCM and its sensitivity to the thermohaline surface forcing, *J. Phys. Oceanogr.*, *23*, 731–757.

Middelburg, J. J., K. S. Soetaert, and P. M. J. Herman (1997), Empirical relationships for use in global diagenetic models, *Deep Sea Res., Part I*, *44*(2), 327–344.

Morse, J. W. (1978), The distribution and forms of phosphorus in North Atlantic deep-sea and continental slope sediments, *Limnol. Oceanogr.*, *23*, 825–830.

Mort, H. P., T. Adatte, K. B. Föllmi, G. Keller, P. Steinmann, V. Matera, Z. Berner, and D. Stuben (2007), Phosphorus and the roles of productivity and nutrient recycling during oceanic anoxic event 2, *Geology*, *35*(6), 483–486.

Murray, R. W., and M. Leinen (1993), Chemical transport to the seafloor of the equatorial Pacific Ocean across a latitudinal transect at 135°W: Tracking sedimentary major, trace, and rare earth element fluxes at the equator and the Intertropical Convergence Zone, *Geochim. Cosmochim. Acta*, *57*, 4141–4163.

Nederbragt, A. J., J. Thurow, H. Vonhof, and H.-J. Brumsack (2004), Modeling oceanic carbon and phosphorus fluxes: Implications for the cause of the last Cenomanian oceanic anoxic event (OAE2), *J. Geol. Soc. London*, *161*, 721–728.

Oschlies, A., K. G. Schulz, U. Riebesell, and A. Schmittner (2008), Simulated 21st century increase in oceanic suboxia by CO_2-enhanced biotic carbon export, *Global Biogeochem. Cycles*, *22*, GB4008, doi:10.1029/2007GB003147.

Poulton, S. W., and D. E. Canfield (2006), Co-diagenesis of iron and phosphorus in hydrothermal sediments from the southern East Pacific Rise: Implications for the evaluation of paleoseawater phosphate concentrations, *Geochim. Cosmochim. Acta*, *70*, 5883–5898.

Ruttenberg, K. C. (1993), Reassessment of the oceanic residence time of phosphorus, *Chem. Geol.*, *107*, 405–409.

Ruttenberg, K. C., and R. Berner (1993), Authigenic apatite formation and burial in sediments from non-upwelling continental margin environments, *Geochim. Cosmochim. Acta*, *57*, 991–1007.

Schenau, S. J., C. P. Slomp, and G. J. De Lange (2000), Phosphogenesis and active phosphorite formation in sediments from the Arabian Sea oxygen minimum zone, *Mar. Geol.*, *169*, 1–20.

Schenau, S. J., G. J. Reichart, and G. J. de Lange (2005), Phosphorus burial as a function of paleoproductivity and redox conditions in Arabian Sea sediments, *Geochim. Cosmochim. Acta*, *69*, 919–931.

Seiter, K., C. Hensen, J. Schroter, and M. Zabel (2004), Organic carbon content in surface sediments-defining regional provinces, *Deep Sea Res., Part I*, *51*, 2001–2026.

Seiter, K., C. Hensen, J. Schroter, and M. Zabel (2005), Benthic carbon mineralization on a global scale, *Global Biogeochem. Cycles*, *19*, GB1010, doi:10.1029/2004GB002225.

Shaffer, G., S. M. Olsen, and J. O. P. Perdersen (2009), Long term oxygen depletion in response to carbon dioxide emissions from fossil fuels, *Nature*, *2*, 105–108.

Six, K., and E. Maier-Reimer (1996), Effect of carbon dynamics on seasonal carbon fluxes in an ocean general circulation model, *Global Biogeochem. Cycles*, *10*, 559–583.

Slomp, C. P., and P. Van Cappellen (2007), The global marine phosphorus cycle: Sensitivity to oceanic circulation, *Biogeosciences*, *4*, 155–171.

Slomp, C. P., E. H. G. Epping, W. Helder, and W. Van Raaphorst (1996), A key role for iron bound phosphorus in authigenic apatite formation in North Atlantic continental platform sediments, *J. Mar. Res.*, *54*, 1179–1205.

Slomp, C. P., J. Thomson, and G. J. de Lange (2002), Enhanced phosphorus regeneration during formation of the most recent eastern Mediterranean sapropel (S1), *Geochim. Cosmochim. Acta*, *66*, 1171–1184.

Stramma, L., G. C. Johnson, J. Sprintall, and V. Mohrholz (2008), Expanding ocean-minimum zones in the tropical oceans, *Science*, *320*, 655–658.

Takahashi, T., W. S. Broecker, and S. Langer (1985), Redfield ratio based on chemical data from isopycnal surfaces, *J. Geophys. Res.*, *90*, 6907–6924, doi:10.1029/JC090iC04p06907.

Tamburini, F., K. B. Föllmi, T. Adatte, S. M. Bernasconi, and P. Steinmann (2003), Sedimentary phosphorus record from the Oman margin: New evidence of high productivity during glacial periods, *Paleoceanography*, *18*(1), 1015, doi:10.1029/2000PA000616.

Tribovillard, N., P. Recourt, and A. Trentesaux (2010), Bacterial calcification as a possible trigger for francolite precipitation under sulfidic conditions, *C. R. Geosci.*, *342*, 27–35, doi:10.1016/j.crte.2009.10007.

Tromp, T. K., P. Van Cappellen, and R. M. Key (1995), A global model for the early diagenesis of organic carbon and organic phosphorus in marine sediments, *Geochim. Cosmochim. Acta*, *59*, 1259–1284.

Tsandev, I., and C. P. Slomp (2009), Modeling phosphorus cycling and carbon burial during Cretaceous Oceanic Anoxic Events, *Earth Planet. Sci. Lett.*, *286*, 71–79.

Tyrrell, T. (1999), The relative influences of nitrogen and phosphorus on oceanic primary productivity, *Nature*, *400*, 525–531, doi:10.1038/22941.

Van Cappellen, P., and R. A. Berner (1988), A mathematical model for the early diagenesis of phosphorus and fluorine in marine sediments: Apatite precipitation, *Am. J. Sci.*, *288*, 289–333.

Van Cappellen, P., and E. D. Ingall (1994), Benthic phosphorus regeneration, net primary production, and ocean anoxia: A model of the coupled marine biogeochemical cycles of carbon and phosphorus, *Paleoceanography*, *9*, 677–692.

Van Cappellen, P., and R. Y. Wang (1996), Cycling of iron and manganese in surface sediments: A general theory for the coupled transport and reaction of carbon, oxygen, nitrogen, sulfur, iron, and manganese, *Am. J. Sci.*, *296*, 197–243.

Van der Zee, C., C. P. Slomp, and W. Van Raaphorst (2002), Authigenic P formation and reactive P burial in sediments of the Nazare Canyon on the Iberian margin (NE Atlantic), *Mar. Geol.*, *185*, 379–392.

Wallmann, K. (2003), Feedbacks between oceanic redox states and marine productivity: A model perspective focused on benthic phosphorus cycling, *Global Biogeochem. Cycles*, *17*(3), 1084, doi:10.1029/2002GB001968.

Wheat, C. G., R. A. Feely, and M. J. Mottl (1996), Phosphate removal by oceanic hydrothermal processes: An update of the phosphorus budget in the oceans, *Geochim. Cosmochim. Acta*, *59*, 3593–3608.

Whitney, F. A., H. J. Freeland, and M. Robert (2007), Persistently declining oxygen levels in the interior waters of the eastern subarctic Pacific, *Prog. Oceanogr.*, *75*, 179–199.

C. Heinze, Geophysical Institute, University of Bergen, Allegaten 70, N-5007, Bergen, Norway.

V. Palastanga and C. P. Slomp, Department of Earth Sciences-Geochemistry, Faculty of Geosciences, Utrecht University, Budapestlaan 4, Utrecht, NL-3584 CD, Netherlands. (v.palastanga@geo.uu.nl)